Turkish Journal of Earth Sciences (Turkish J. Earth Sci.), Vol. 18, 2009, pp. 55–83. *Copyright ©TÜBİTAK*
doi:10.3906/yer-0806-8 First published online 23 July 2008

Whole Rock and Mineral Chemistry of Ultramafic-mafic Cumulates from the Orhaneli (Bursa) Ophiolite, NW Anatolia

ENDER SARIFAKIOĞLU[1], HAYRETTİN ÖZEN[2] & JOHN A. WINCHESTER[3]

[1] General Directorate of Mineral Research and Exploration, Department of Geology, TR–06520 Ankara, Turkey
(E-mail: esarifakioglu@mta.gov.tr)

[2] General Directorate of Mineral Research and Exploration, Department of Mineral Research and Exploration, TR–06520 Ankara, Turkey

[3] Keele University, School of Physical and Geographical Sciences, ST5 5BG Staffordshire, England

Received 23 June 2007; revised typescript received 24 November 2007; accepted 07 December 2007

Abstract: The Orhaneli ophiolite, situated in the western part of the İzmir-Ankara-Erzincan Suture Zone (İAESZ) and south of Bursa, exposes cumulates belonging to the mantle-crust transition zone. The Orhaneli ophiolite consists mainly of ultramafic cumulates and subordinate mafic cumulates. The basal cumulate sequence comprises dunites locally interlayered with chromitite levels. Above, dunitic cumulates, commonly interbanded with cumulate wehrlites, grade up into two pyroxene peridotites (cumulate lherzolites showing some transition to cumulate harzburgites in places). The observation of cumulate gabbroic thin layers intercalated with ultramafic cumulates at least three times suggests that the magma chamber was periodically replenished by basaltic liquids. Petrographic studies show that the crystallization orders in the mafic-ultramafic cumulates follow two lines: (1) sp-ol-cpx-plag (chromitite, dunite, wehrlite, pyroxenite, gabbro), (2) sp-ol-cpx-opx-plag (chromitite, dunite, wehrlite, lherzolite, harzburgite, pyroxenite, gabbro).

Geochemical analysis has shown that Th enrichment within the LILE (K, Sr, Rb, Ba) group and the depletion of HFSE (Ti, Nb, Zr, Y) relative to MORB indicate a suprasubduction zone tectonic setting for the formation of the Orhaneli ophiolite. The cumulate gabbroic rocks show low Ti (<1%) and Zr (<50 ppm) and very low Ti (<0.2%) and Zr (<8 ppm) while isolated diabases have low TiO_2 (0.72–0.87%) and Zr (<55 ppm). Mineral compositions, notably olivine ($Fo_{81–93}$), clinopyroxene ($Mg\#_{83–94}$), orthopyroxene ($Mg\#_{77–92}$), plagioclase ($An_{86–99}$) and Cr-spinel ($Cr\#_{0.40–0.73}$) also indicate that the Orhaneli ophiolite is a suprasubduction zone (SSZ) type.

Field and petrochemical studies suggest that the Orhaneli ophiolite formed as a product of island arc tholeiitic (IAT) and/or boninite-like magmatism in an intraoceanic suprasubduction zone system, similar to other Neotethyan Ophiolites, within the northern branch of the Neotethys Ocean, probably in the forearc region.

Key Words: Mantle-crust transition zone, mafic-ultramafic cumulates, magmatic recycling, magma chamber, crystallization order, SSZ-type ophiolite, Turkey

Orhaneli (Bursa) Ofiyolitindeki Ultramafik-mafik Kümülatların Kaya ve Mineral Kimyası, KB Anadolu

Özet: İzmir-Ankara-Erzincan Kenet Zonu'nun (İAEKZ) batı kısmında, Bursa'nın güneyinde bulunan Orhaneli ofiyoliti, manto-kabuk geçiş zonuna ait başlıca ultramafik kümülatlardan ve daha az mafik kümülatlardan oluşur. Kümülat istif, kümülat dunitler ile başlar. Yer yer değişik kalınlıktaki kromitit seviyelerle ardalanmalıdır. Dunitik kümülatlar, başta verlitler olmak üzere magmatik tabakalanma sunarken bazen iki piroksenli kümülat peridotitlerle (yer yer harzburjitlerle geçişli lerzolit) ardalı magmatik seviyeler oluşturur. Ultramafik kümülatlarla en az üç kez ardalanmalı ince gabro seviyelerinin izlenmesi, kümülatların oluşumunda magma odasının bazaltik akışkanlar tarafından periyodik olarak (magmatik döngü) beslendiğini gösterir. Mafik-ultramafik kümülatların petrografik özelliklerine göre bu kayaçların oluşumunda etkili olan kristalizasyon sırasının iki şekilde olduğu anlaşılmıştır: (1) sp-ol-cpx-plag (kromitit, dunit, verlit, piroksenit, gabro), ve (2) sp-ol-cpx-opx-plag (kromitit, dunit, verlit, lerzolit, harzburjit, piroksenit, gabro).

Jeokimyasal verilere göre K, Sr, Rb, Ba elementleri (LILE) bazik kayaçların (katmanlı gabrolar, izole diyabaz dayklar) okyanus tabanı hidrotermal alterasyona maruz kalmasından dolayı değişken bir dağılım sunarken Th elementinde zenginleşmenin ve HFS elementlerininde (Ti, Nb, Zr, Y) tüketilmenin izlenmesi Orhaneli ofiyolitinin dalma-batma zonu üstü (supra-subduction zone) tektonik ortamda oluştuğunu gösterir. Kümülat gabrolar, düşük TiO_2 (<%1) ve Zr (<50 ppm) ve çok düşük TiO_2 (<%0.2) ve Zr (<8 ppm) içerikleri sergilerken, izole diyabazların TiO_2 (%0.72–0.93) ve Zr (<55 ppm) içeriği düşüktür. Mafik-ultramafik kümülatlardaki olivin ($Fo_{81–93}$), klinopiroksen ($Mg\#_{83–94}$), ortopiroksen ($Mg\#_{77–92}$), plajiyoklas ($An_{86–99}$) ve Cr-spinel ($Cr\#_{0.40–0.73}$) bileşimi SSZ-tipi ofiyolitlerini işaret eder.

Arazi ve petrokimyasal çalışmalar, Orhaneli ofiyolitinin İAEKZ boyunca gözlenen diğer Neotetis ofiyolitleri gibi Neotetis okyanusunun kuzey kolunda, okyanus içi dalma-batma zonu sistemi içerisinde, yay önü tektonik ortamda ada yayı toleyit (IAT) ve/veya boninit benzeri magmadan oluştuğunu göstermektedir.

Anahtar Sözcükler: Manto-kabuk geçiş zonu, mafik-ultramafik kümülatlar, magmatik döngü, magma odası, kristalizasyon sırası, SSZ-tipi ofiyolitler, Türkiye

Introduction

The Orhaneli (Bursa) ophiolite is situated in northwestern Anatolia, on the western section of the 2600-km-long İzmir-Ankara-Erzincan Suture Zone (Figure 1), which forms the tectonic boundary between the Pontides in the north and the Anatolide-Tauride platform in the south and is marked by ophiolitic bodies. The Orhaneli ophiolite and the other nearby ophiolites, such as the Harmancık (Bursa), Tavşanlı (Kütahya) and Dağküplü-Mihalıççık (Eskişehir) ophiolites, are the remnants of the İzmir-Ankara-Erzincan Ocean, the local term for the northern branch of the Neotethys Ocean.

Özkoçak (1969) undertook the first detailed fieldwork on the Orhaneli ophiolite. He stated that the peridotites were formed by the intrusion of ultrabasic magma during the Late Cretaceous. Lisenbee (1972), on the other hand, proposed that the Orhaneli massif was emplaced as a solid mass during the Late Cretaceous. Emre (1986) differentiated tectonite harzburgite-dunites, cumulate harzburgite-dunites and pyroxenite gabbro units in the Orhaneli ophiolite and Tankut (1991) stated that the Orhaneli massif comprised ultrabasic rocks formed by the differentiation of upper mantle and gabbros observed locally. Gültaşlı (1996) argued that the ultramafic-mafic rocks of the Orhaneli ophiolite were formed by ocean floor spreading and emplaced by thrusting during the Late Cretaceous. Sarıfakıoğlu & Gültaşlı (2003) pointed out that the petrochemical features of the mafic rocks in the Orhaneli ophiolite indicate that it is a suprasubduction zone type ophiolite. Örgün *et al.* (2004) discussed the suitability of the olivine crystals in the Orhaneli dunites for use as steel slag conditioner, foundry sand and abrasives.

In an ophiolitic sequence which is a remnant of oceanic lithosphere, pillow lavas, sheeted dike complex, mafic-ultramafic igneous rocks representing the oceanic crust and mantle peridotites are typically observed. The most important feature of the Orhaneli ophiolite which distinguishes it from other ophiolitic bodies in the region is its inclusion of the mafic-ultramafic cumulates that belong to the transition zone between the oceanic crust and subjacent upper mantle, and indicate the petrographic MOHO.

The purpose of this study is to discuss the geology of the ultramafic cumulates interlayered with thin gabbroic layers in the field and to understand their magmatic evolution by studying the gradual transitions and interlayering in them, and to evaluate the petrogenetic processes by means of petrographic/geochemical studies, thereby providing a new look at its geodynamical setting.

Geological Background

The Orhaneli ophiolite is situated 20 km south of Bursa and is approximately 50-km long, 15-km wide and 1500-m thick (Figures 2 & 3). Whereas the main ophiolite slab was thrust southwards over Cretaceous blueschists and marbles of the Anatolide-Tauride Platform, it was also emplaced by north-directed backthrusting on to Upper Triassic deformed graywackes containing Permo–Carboniferous limestone blocks and the Jurassic Bilecik Limestone in the Sakarya zone.

While Harris *et al.* (1994) obtained an age of 101±4 Ma by means of Ar-Ar dating on the garnet-amphibolite metamorphic sole below the ophiolitic slab, Ar-Ar dating on the metamorphic sole rocks from the basement of the Tavşanlı (Kütahya) ophiolites yielded an age of 93±2 Ma (Önen & Hall 2000).

The ophiolitic tectonic mélange locally observed along the thrust zones below the Orhaneli ophiolite includes serpentinite, radiolarite, limestone and mafic rock blocks. Palaeontological studies on the pelitic rocks that form the matrix of the tectonic mélange suggest a Late Cretaceous age of mélange formation (Özkoçak 1969).

The Upper Cretaceous Orhaneli ophiolite is an assemblage of cumulate peridotite and gabbro that belongs to the mantle-crust transition (Figures 4 & 5). Dunites (60%) and pyroxene-bearing peridotites (30%), such as wehrlites, lherzolites and harzburgites representing the lower oceanic crust are observed as ultramafic cumulates. The proportion of pyroxenites formed almost entirely of pyroxene minerals is about 5%. Cumulate gabbros and gabbronorites are less abundant than the ultramafic cumulates.

The magmatic layering of cumulate peridotites and gabbros and a few cm–m-thick chromite bands display a N–S strike and a dip of 55–88° to the west, suggesting that the basement of the Orhaneli ophiolite is situated in the eastern part of the slab. If so, the peridotite sequence begins with dunites at the base, which are generally interlayered with pyroxene-bearing peridotites, mostly wehrlites and lherzolites on various scales ranging from 1 cm to 150 m (Figure 6a, b). In the western part of the

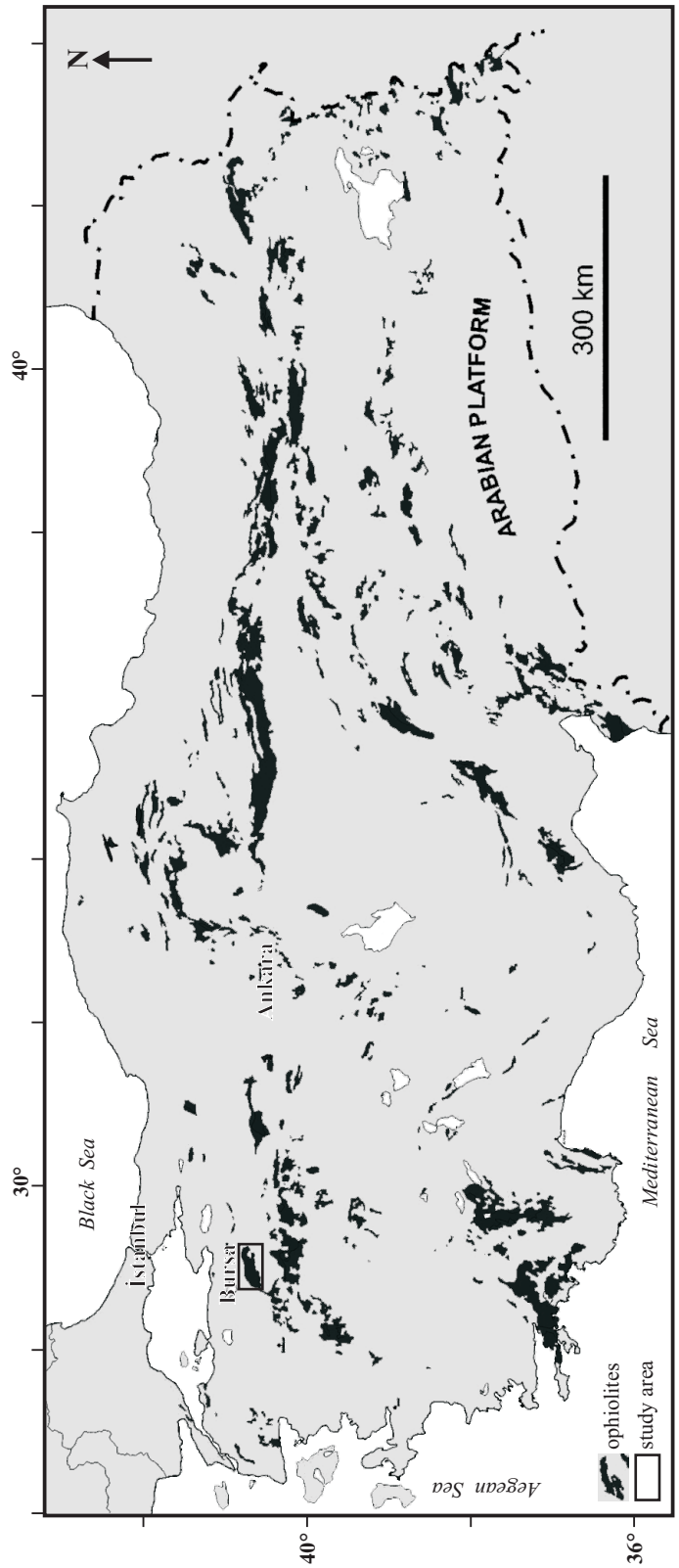

Figure 1. Distribution of the Neotethyan Ophiolites in Turkey and location of the studied area (from Şenel 2001).

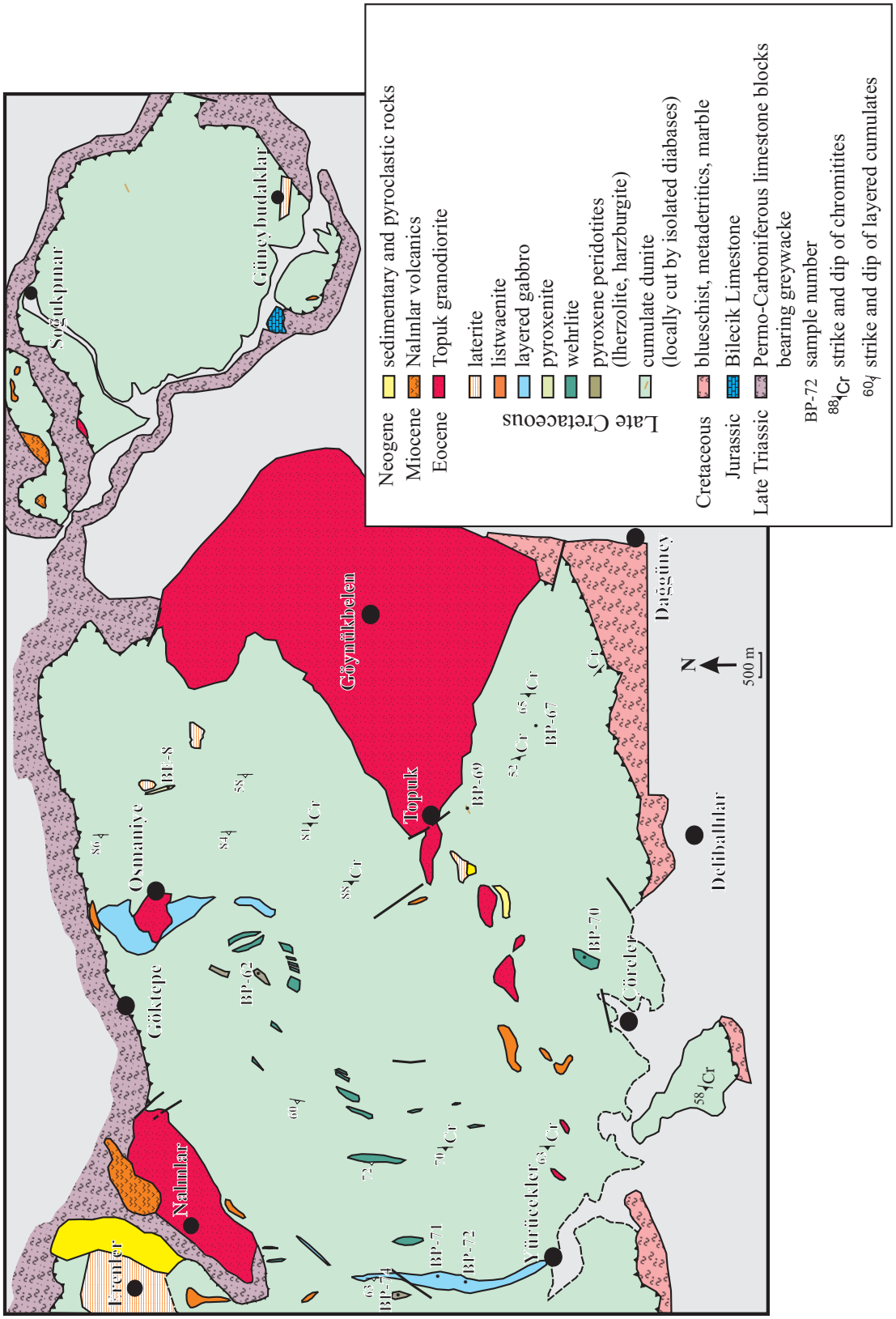

Figure 2. The geological map of the eastern Orhaneli ophiolite (Özen *et al.* 2004).

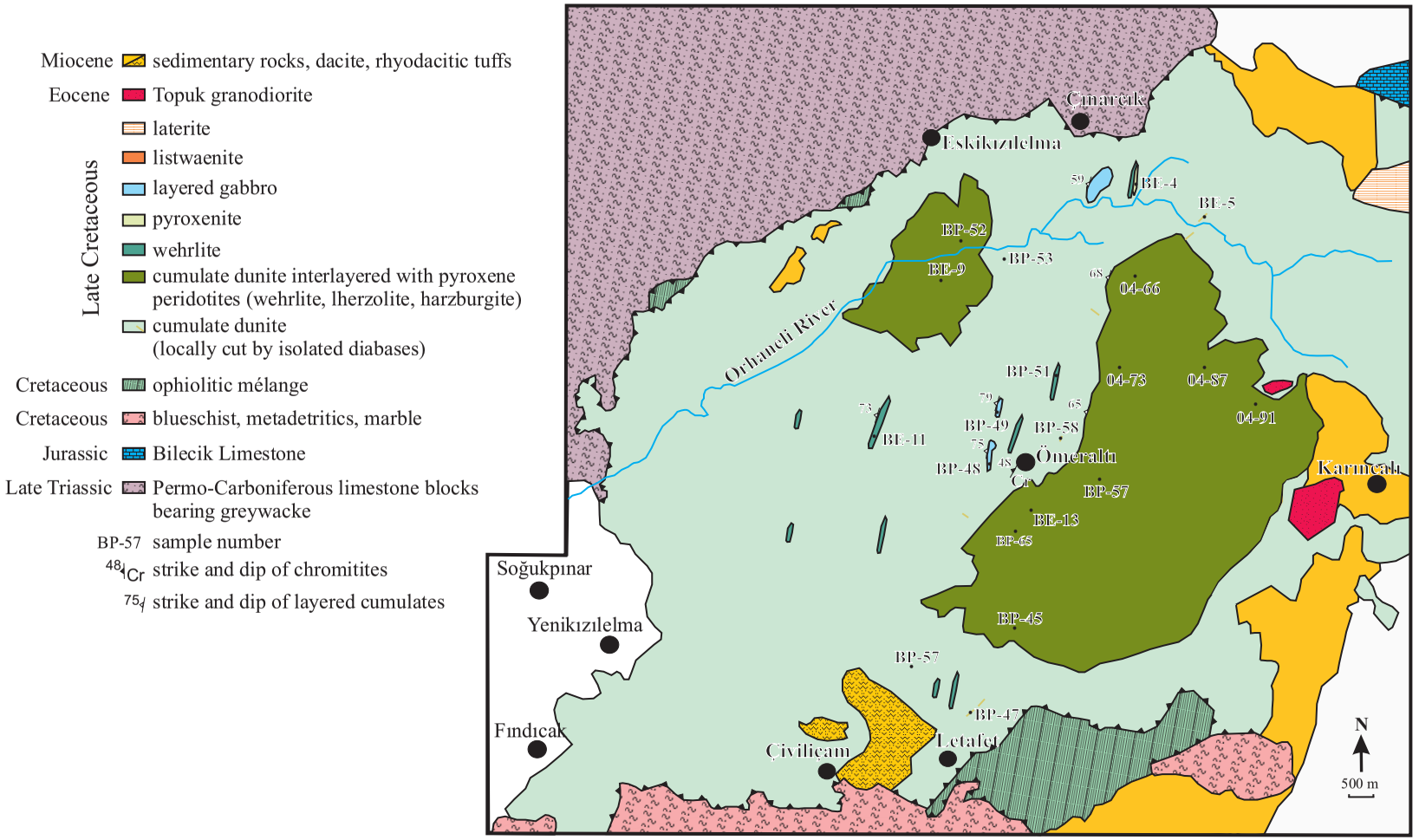

Figure 3. The geological map of the western Orhaneli ophiolite (Özen *et al.* 2004).

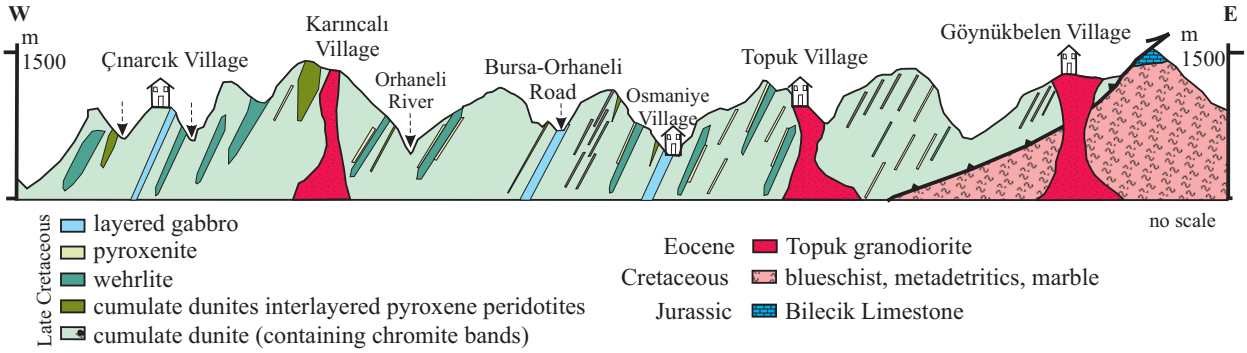

Figure 4. Generalized geological cross-section from east to west of the Orhaneli ophiolite (Özen *et al.* 2004).

slab, pyroxene-bearing peridotites (wehrlite, lherzolite, harzburgite, and pyroxenite) cover wide areas and display both lateral and vertical gradual transitions (Figure 6c).

The cumulate peridotites are locally cut by isolated diabase dykes 0.5–3 m thick, which are discontinuous owing to the tectonic deformation related to the ophiolite emplacement. These dykes have been partially rodingitised (Figure 6d).

The mafic cumulates observed at three field localities and confined to a restricted area occur as layered gabbros and gabbronorites (Figure 6e). The mafic-ultramafic cumulate sequence situated between the gabbroic cumulates shows at least three repetitive cycles (Figure 4). Cumulate gabbros observed to form thin interbeds within the ultramafic layered units and cumulate recycling are interpreted as the result of periodic replenishment of the magma chamber.

At the base of the ultramafic cumulates alteration zones were developed. These include lateritic zones up to 10 m thick on the dunites, which display a subdued topography (Özen *et al.* 2005). Carbonatized and silicified serpentinites (listwaenites) also occur along shear zones in the ultramafic rocks and the basal thrust zone of the ophiolitic slab.

The General Directorate of Mineral Research and Exploration (MTA) has been carrying out studies of ore formation related to the ophiolites in the region for more than 30 years. As a result of these studies, the Harmancık (Bursa) ophiolite 20 km south of the study area which contains mantle ultramafic rocks (harzburgite, dunite) and the Orhaneli (Bursa) ophiolites comprising mostly mafic-ultramafic cumulates are considered to be parts of a single unit (Y.Z. Özkan, personal communication 2005).

The Topuk granodiorite, which cuts both metamorphic rocks of the Tavşanlı Zone and ophiolitic rocks, was originally recorded as Eocene (53 to 48 Ma) (Harris *et al.* 1994). Field studies and geochronological data suggest that these ophiolites, which are the remnants of the northern branch of the Neotethys Ocean, were emplaced during the Late Cretaceous–Paleocene as discrete fragments as a result of the collision of the Sakarya Zone, forming the southern part of the Pontides, and the Anatolide platform (Okay *et al.* 2001).

Petrography

The mantle-crust transition zone is marked by a cumulate peridotite-gabbro assemblage, which separates upper mantle peridotites from crustal isotropic gabbros. This transition zone indicates that the former petrological Moho is preserved in the area. In this zone, ultramafic rocks dominate as lower crustal cumulates. The dunites at the base of the magmatic sequence grade up into pyroxene-bearing peridotites, commonly wehrlites, with less abundant lherzolites and scarce harzburgites. Cumulate gabbros occur rarely. The mafic-ultramafic cumulate rocks are cut by isolated diabases in places.

Dunites

The dunites display adcumulate texture and consist almost entirely of thin–medium rounded olivine crystals (Figure 7a). The olivine crystals have been partially or completely serpentinized. In some extensively serpentinized dunites, magnetite also occurs, principally as finely disseminated grains in a mesh texture within the serpentine minerals.

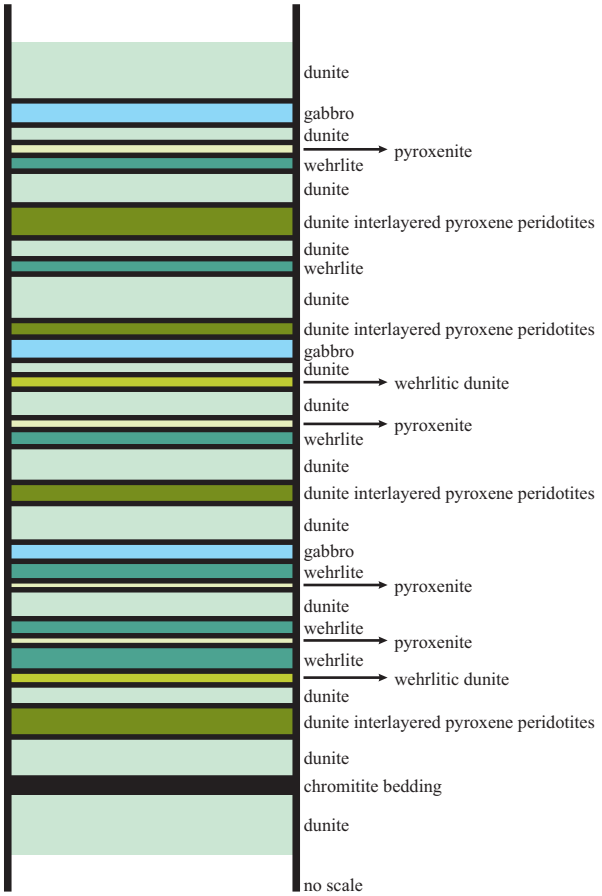

Figure 5. The illustrated stratigraphic log of the ultramafic-mafic cumulates from the Orhaneli Ophiolite.

Cr-spinel is present in lesser amounts. Dunites sometimes show a foliation or lineation defined by economic Cr-spinel layers up to 0.5–8 m thick and 100–250 m long. The chromite- and olivine-rich layers show rhythmic repetitions in these zones. The dunites are interlayered with clinopyroxene-rich wehrlitic dunites and/or wehrlites on various scales (3 cm–150 m) (Figure 7b). Yet more pyroxene-rich rocks, namely pyroxenites (clinopyroxenites), were observed as lenses or bands up to 2–4 cm wide embedded in dunites. During the crystallization from dunites to wehrlites and clinopyroxenites, the order of crystallization is: spinel, spinel + olivine; olivine; olivin + clinopyroxene, clinopyroxene.

Wehrlite

The wehrlites, which are more abundant than the other peridotitic cumulates, contain olivine (45–80%) and clinopyroxene (20–25%) displaying mesocumulate texture (Figure 7c). The partly serpentinized cumulus olivine crystals vary greatly in size within thin-sections (from 100 μm to 1 mm). The partly uralitized clinopyroxenes as post-cumulus crystals range in size from 0.2 mm to 5 mm. Some wehrlites display alternating irregular bands with 1 to 10 mm width of olivine and clinopyroxene crystals. However, wehrlites grade into clinopyroxenite with a decrease in the proportion of olivine to clinopyroxene.

Lherzolite

The cumulate dunites are locally interlayered with lherzolite layers. However, in the west of the Orhaneli ophiolitic slab, where the cumulate dunites and the pyroxene-bearing peridotites coexist, lherzolites were observed subordinate to the wehrlites, a relationship similar to that in the Semail Ophiolite which displays the cumulate peridotite-gabbro assemblage of the mantle-crust transition zone in the Cretaceous Neotethyan Ophiolite Belt (Osman 2004). The peridotites contain 80% olivine and 20% pyroxene crystals (Figure 7d). Both orthopyroxenes (enstatite) and clinopyroxenes (diopside) are present. Post-cumulus pyroxene crystals among the small- to medium-sized cumulus olivine crystals may be up to 10 mm across. The two pyroxene crystal rich bands within the lherzolite have been defined as websterites: the medium-coarse pyroxene crystals display adcumulate texture. Chrome spinel crystals, ranging in size from 0.1–2 mm, are rare accessory minerals. The crystallization order in two pyroxene-bearing peridotites is spinel; olivine; clinopyroxene; orthopyroxene.

Harzburgite

The occurrence of harzburgite is similar to that in the Ordovician Bay of Islands Ophiolite in Canada (Bedard 1991), with dunite, wehrlite, harzburgite, lherzolite and olivine websterite occurring as peridotitic cumulates. It may also resemble the Mesozoic ophiolites in the Koryak Mountains in Russia (Ishiwatari *et al.* 2003) in containing iron-rich harzburgite, dunite, orthopyroxenite and websterite. The cumulate dunites in the Orhaneli Ophiolite locally contain rounded orthopyroxene grains and grade into harzburgitic cumulates (Figure 7e). In thin to medium grained harzburgites, 85% olivine and 10–15% orthopyroxene crystals are present. The olivine crystals are partially serpentinized whereas the orthopyroxene crystals

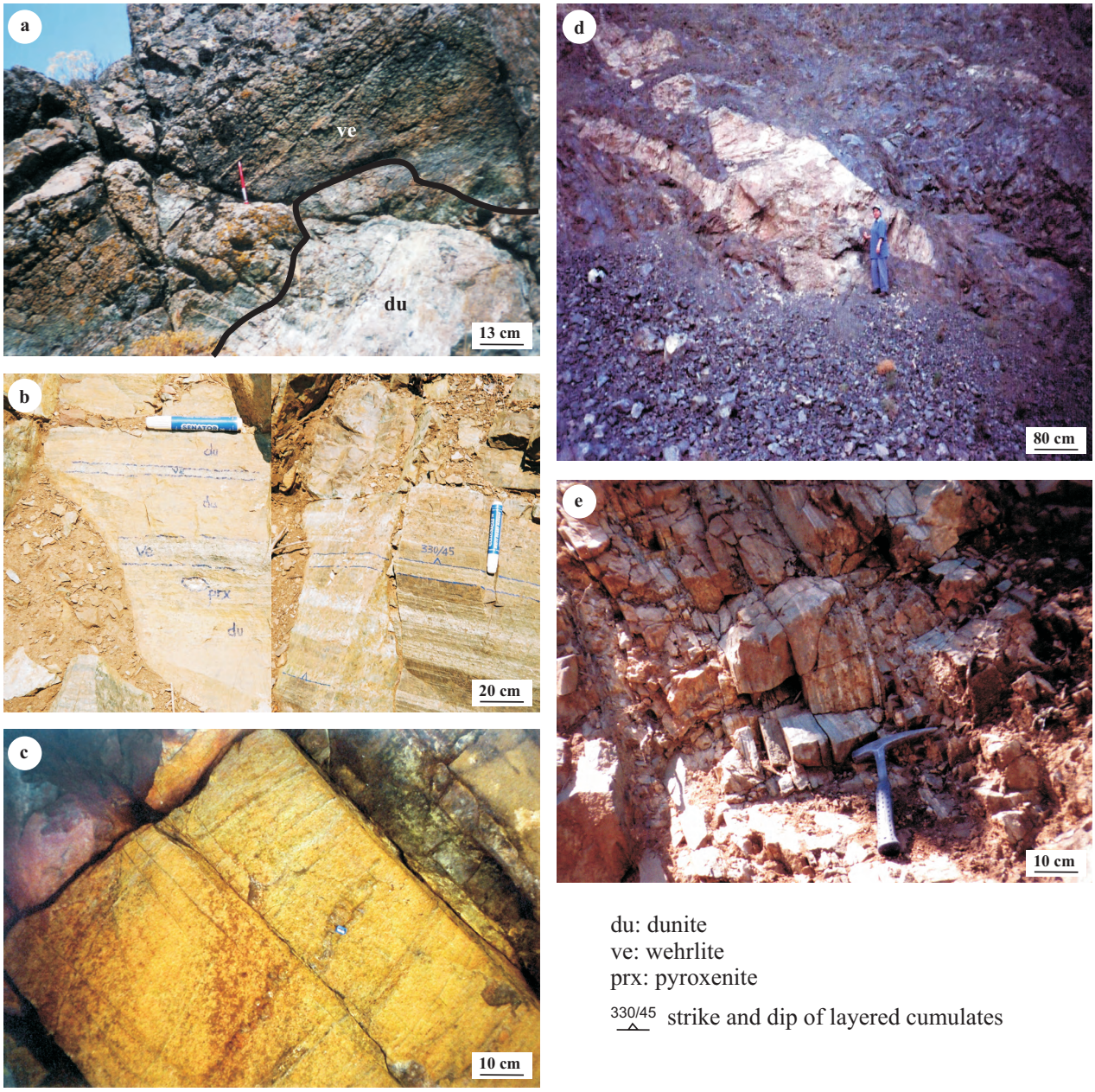

Figure 6. (a) The wehrlite containing pyroxenite veins in the serpentinized cumulate dunite; (b) layering in the ultramafic cumulates; (c) the rods of pyroxenite in wehrlitic dunite; (d) view of a rodingite dyke in the cumulate peridotites; (e) the pyroxene-rich (grey) and the plagioclase-rich (light) levels from the mineral-graded layers in the cumulate gabbros.

appear as bastite pseudomorphs of orthopyroxene. Accessory chromite forms up to 2–3% of the rock. In the field, harzburgites are scarcer than other pyroxene-bearing peridotites, and appear as lenses (~100 m) within cumulate dunites and may grade into lherzolites.

Gabbroic Rocks

The gabbroic rocks form thin interbeds within the cumulate dunites of the lower crust. The fine-grained (ranging from 0.3 mm to 0.6 mm in size) layered gabbros are formed by the rhythmic repetition of layers 1–3 cm

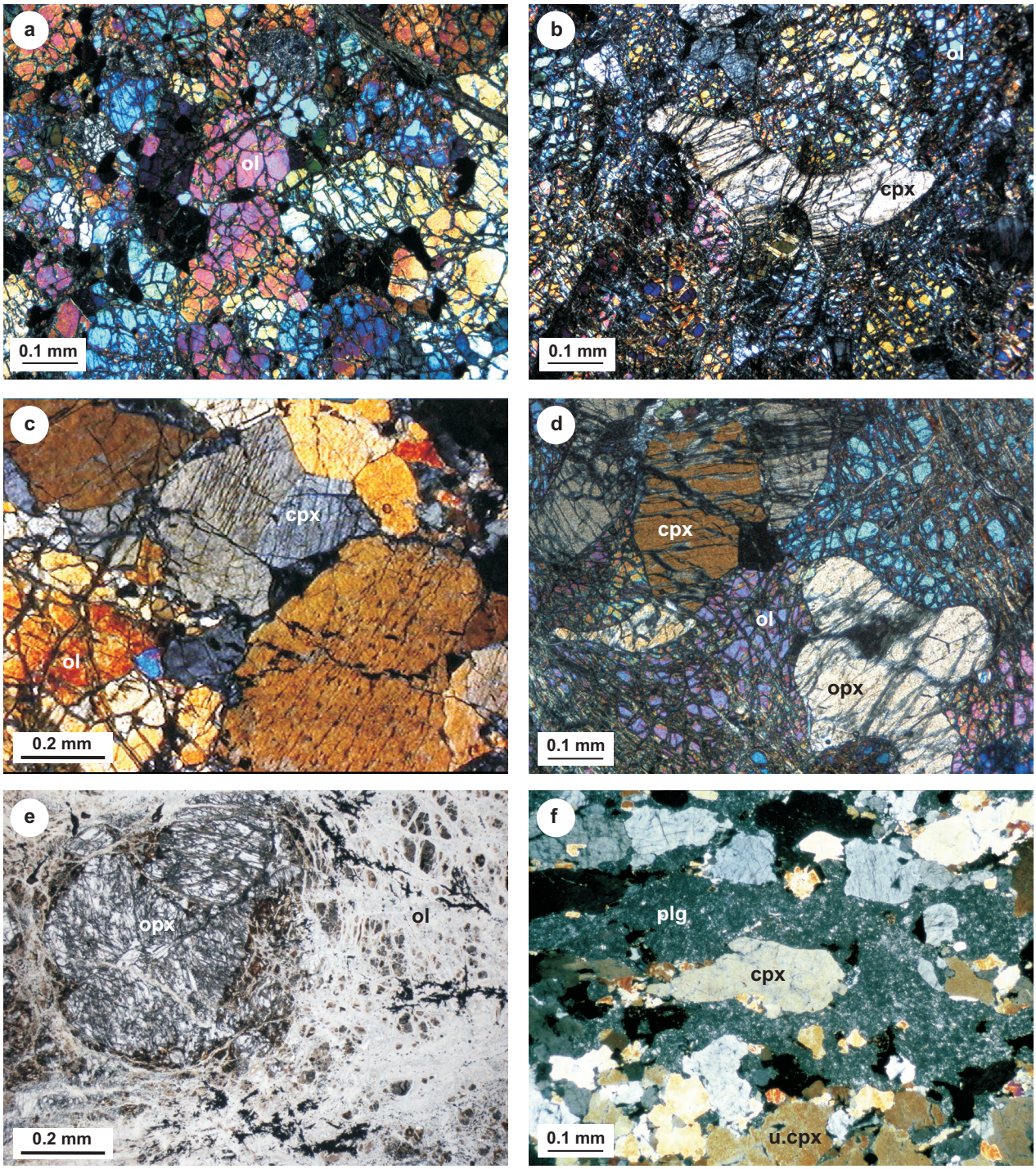

Figure 7. Photomicrographs (crossed and planar polars) of ultramafic cumulates in the Orhaneli ophiolite: **(a)** adcumulate texture consisting of rounded olivine crystals in cumulate dunite; **(b)** intersertal pyroxene crystals between cumulus olivine crystals in wehrlitic dunite; **(c)** olivine-clinopyroxene mesocumulate texture from wehrlite; **(d)** cumulus olivine crystals and postcumulus pyroxene crystals in lherzolite; **(e)** heteradcumulate texture in harzburgite consisting of rounded orthopyroxene grains enclosed in olivine crystals and **(f)** planar lamination of uralitized clinopyroxene and saussuritized plagioclase crystals in the layered gabbros (ol– olivine, cpx– clinopyroxene, opx– orthopyroxene, plg– plagioclase, u.cpx– uralitized clinopyroxene).

thick bearing alternately dominant felsic minerals and mafic minerals (Figure 7f).

They include 50–55% cumulus plagioclase and 40–45% cumulus clinopyroxene. Green spinels (hercynite) (up to 3%) occur as intercumulus crystals. The layered gabbros displaying adcumulate texture have been partially or completely altered, with clinopyroxene replaced by actinolite (uralitization) and chlorite, and plagioclase replaced by chlorite, epidote (saussuritization) and hydrogarnet.

The layered gabbros alternate with the planar-laminated gabbronorites. The gabbronorites display plagioclase + clinopyroxene + orthopyroxene adcumulate texture. They include 60–65% plagioclase, 20–25% clinopyroxene and 5–10% orthopyroxene crystals, ranging in size between 0.1 mm and 1 mm. A few green spinels (hercynite) are present as intercumulus crystals.

Isolated Diabase Dykes

The diabases cutting the layered ultramafic cumulates display subophitic or intergranular textures. The fine-grained diabases have usually been metamorphosed to greenschist grade beneath the ocean-floor. While the primary plagioclase (labradorite) is replaced by albite, epidote, chlorite and sericite, the clinopyroxene was uralitized and replaced by actinolite. Sometimes, the diabase dykes have been almost completely altered to rodingites containing secondary minerals such as hydrogarnet pseudomorphs after plagioclase, and chlorite and tremolite replacing clinopyroxene.

Analytical Method

Of the mafic-ultramafic rock samples collected from the northern Orhaneli (Bursa) ophiolite, 38 samples were analysed for major and trace elements. 27 of these analyses were used in geochemical evaluation because some trace element concentrations were found to be below the instrument detection limits (Table 1). All analyses were performed at Keele University, England, using an ARL 8420 X-ray Fluorescence spectrometer, calibrated against both international and internal Keele standards of appropriate composition (Floyd & Castillo 1992). Analytical methods and precision have been described in Winchester *et al.* (1992).

The chemical compositions of olivine, clinopyroxene, orthopyroxene and Cr-spinel from ultramafic layered cumulates and plagioclase, clinopyroxene and orthopyroxene from gabbroic rocks have been determined by microprobe analysis, carried out using the Cameca SX–50-type electron microprobe at the Department of Petrology in Pierre and Marie Curie University, Paris. Operating conditions were: 15 kV accelerating voltage, 12 nA current and 10s counting time per each element. Results of microprobe analyses are given in Tables 2 to 9.

Whole Rock Chemistry

The results of the major and trace element analyses related to the mafic-ultramafic cumulates and isolated diabase dykes are given in Table 1. Of the ultramafic cumulates, dunites locally observed lherzolites and harzburgites which are observed to grade into each other in the field, include more LOI than wehrlites and pyroxenites. While the LOI in the dunites, harzburgites and lherzolites due to serpentinization is ~10%, it ranges between 1–7% in wehrlites and pyroxenites. This indicates that peridotites with higher olivine content are more sensitive to serpentinization rather than those with higher pyroxene content. LOI varies between 0.57–3.99% in mafic gabbros and diabase dykes: its enhancement probably results from low-grade oceanic hydrothermal alteration. We suggest that this alteration also caused mobility and expulsion of some large-ion-lithophile (LIL) elements (Hart *et al.* 1974; Humphris & Thompson 1978).

Since the MgO (30–47wt%) content of the rocks of the ultramafic cumulates of the Orhaneli ophiolite is high, except in the pyroxenites, they fall in the field of HOT (Harzburgite Ophiolite Type) on an Al_2O_3-CaO-MgO diagram (Figure 8a). Pearce (2003) indicated that, in general, mostly LOT (Lherzolite Ophiolite Type) ophiolites have features similar to MORB while depleted HOT ophiolites have features similar to SSZ rocks. Highly depleted and serpentinized peridotites from the Mariana and Tonga Troughs are likewise believed to have formed by hydrous melting of a depleted mantle in island arc environments in intra-oceanic settings (Bloomer & Hawkins 1987; Flower *et al.* 2001). The Al_2O_3, MgO and Na_2O+ K_2O values of the mafic-ultramafic cumulates from the Orhaneli ophiolite have been plotted on the AFM diagram of Beard (1986). The cumulate dunites interlayered with pyroxene peridotitic cumulates plot in the arc-related ultramafic cumulate field, whereas cumulate gabbros are scattered in the arc-related mafic cumulate field (Figure 8b). The major element values of isolated diabases are

similar to the arc-related non-cumulate gabbro and dolerite field. This implies that mafic-ultramafic cumulates and isolated diabases formed in a suprasubductional setting.

Cr, Ti, V, Y, Zr, Nb and Th are normally immobile under conditions of hydrothermal alteration and at intermediate to high grades of metamorphism (e.g., Pearce & Cann 1973; Smith & Smith 1976; Floyd & Winchester 1978). Therefore, the values and ratios of these elements from mafic cumulates and isolated diabases from the Orhaneli ophiolite have been used in trace element discrimination diagrams to define the tectonic setting. The low Nb/Y ratios in gabbros and isolated diabases (0.1–0.8) indicate that they are subalkaline (Winchester & Floyd 1977), while generally the low Ti/V ratio (3–21 in gabbros; 15–20 in diabases) is typical of island arc tholeiites (Figure 9a). The Ti-V diagram for the gabbros and diabases show that three gabbro samples have low Ti and so plot in the boninite field, while the other samples plot within the island arc tholeiite (IAT) field. The dolerite dykes with a negative Nb and Ti anomaly cutting the Harmancık ophiolite, situated south of the Orhaneli ophiolite, are considered to have formed in a suprasubduction zone setting (Bacak & Uz 2003; Manav *et al.* 2004). On a Cr-Y discrimination diagram (Pearce 1982) cumulate gabbros are again divided into those which plot within the IAT and boninite fields (Figure 9b). Diabases, by contrast, cluster in the IAT field. Boninites are defined on a chemical basis and are characterized by very low Ti (<0.3%), Y, Zr, and heavy-rare-earth elements, and are variably enriched in SiO_2 (>55%), MgO (>6%), Ni (70–450 ppm), Cr (200–1800 ppm), large-ion lithophiles, H_2O and light-rare-earth elements. Boninites are generally considered to be a product of subduction zone related melting, especially during the earliest phases of island arc volcanism (Crawford *et al.* 1981; Bloomer & Hawkins 1987; Wilson 1989). Although a few gabbro samples from the Orhaneli ophiolite contain very low Ti, Y and Zr they lack the high SiO_2 of true boninites. The geochemical data of the Orhaneli cumulates and isolated diabases therefore indicate an IAT-type and/or boninite-like sources within suprasubduction zone tectonic setting.

The Nb/Th ratio versus Y diagram (Jenner *et al.* 1991) shows that the gabbroic cumulates and isolated diabases in the Orhaneli ophiolite plot in an arc-related tectonic environment (Figure 10a). The Ti-Zr tectonomagmatic discrimination diagram of (Pearce & Cann 1973) also suggests that the mafic rocks of the Orhaneli ophiolite formed in a suprasubduction zone tectonic setting (Figure 10b). The cumulate gabbros and isolated diabases in the Orhaneli ophiolite thus show similar geochemical characteristics to ophiolites in the other parts of the İAESZ (Göncüoğlu *et al.* 2000; Bacak & Uz 2003; Manav *et al.* 2004; Sarıfakıoğlu *et al.* 2006; Özen *et al.* 2006).

The multi-element diagrams normalized against MORB for the cumulate gabbros and isolated diabases are presented in Figure 11. Enrichment of Th is a relatively stable and reliable indicator despite hydrothermal alteration among the LIL element group (K, Sr, Rb, Ba), with respect to the other incompatible elements. The enrichment of LIL elements relative to HFS elements (Ti, Nb, Zr, Y) has been attributed to LIL-enriched fluids derived from the subducting oceanic slab and requires that the HFS elements are mostly retained in the down-going slab (Wood *et al.* 1979; Pearce 1983; Saunders & Tarney 1984). The depletion of the high field strength (HFS) elements and the enrichment of LIL elements, especially Th, obtained from the Orhaneli ophiolite indicate a suprasubduction zone tectonic environment, suggesting a comagmatic relationship between cumulate gabbros and the isolated diabases which cut them. The Orhaneli ophiolite thus displays a similar tectonic setting to other Late Cretaceous Neotethyan ophiolites in the Eastern Mediterranean Region (Yalınız *et al.* 1996; Elitok 2001; Manav *et al.* 2004; Parlak *et al.* 2006; Çelik *et al.* 2006).

Mineral Chemistry

Olivine

High-Mg olivine (forsterite) was analysed from cumulate peridotites (dunite, wehrlite, lherzolite, harzburgite). Cumulate dunites containing forsterite grade both vertically and horizontally into pyroxene-bearing peridotites, so that while the forsterite component is Fo_{90-92} in lherzolite, it is Fo_{90-93} in harzburgites, and only Fo_{81-82} in wehrlites (Table 2). The NiO content, which varies between 0.5% and 0.1%, also decreases from harzburgites to lherzolites and wehrlites (Table 2). This shows that there is a positive correlation between the forsterite content–as linked to the fractional crystallization of olivine–and the content of NiO. The olivine composition of the ultramafic cumulates of the Orhaneli ophiolites is similar to that of other Eastern Mediterranean ophiolites, such as the Kızıldağ ophiolite (Bağcı *et. al.* 2005), Mersin ophiolite (Parlak *et al.* 1996), Pozantı-Karsantı ophiolite (Parlak *et al.* 2002), Troodos ophiolite (Portnyagin *et al.* 1996) and Semail ophiolite

Table 1. The major-trace element analyses results of mafic-ultramafic cumulates and isolated diabases belonging to the Orhaneli ophiolite.

Sample	BP-47	BP-58B	BP-69	BE5	BP-58D	BP-48	BP-49A	BP-71	BP-72	BP-73	BP-53B	BP-57C	BP-67A	BP-67B
Rock name	diabase	diabase	diabase	diabase	diabase	gabbro	gabbro	gabbro	gabbro	gabbro	dunite	dunite	dunite	dunite
SiO_2	48.44	47.06	50.66	42.89	47.46	46.66	46.68	37.24	42.82	44.14	39.48	40.46	39.77	39.70
TiO_2	0.93	0.72	0.89	0.87	0.79	0.92	0.73	0.15	0.11	0.05	0.00	0.06	0.00	0.01
Al_2O_3	15.42	15.67	16.05	12.86	15.51	16.16	12.67	20.80	19.53	18.78	0.51	0.87	0.42	0.46
$Fe_2O_3^T$	12.26	12.53	8.10	13.40	11.25	12.49	10.48	10.98	8.97	8.23	8.72	9.13	10.21	9.23
MnO	0.17	0.17	0.08	0.21	0.16	0.16	0.16	0.14	0.11	0.10	0.12	0.13	0.14	0.12
MgO	8.03	7.60	8.58	11.81	7.44	7.59	8.73	10.27	9.84	11.75	40.94	37.54	47.18	46.69
CaO	12.08	11.44	10.44	13.73	12.00	10.85	17.06	17.16	14.20	14.62	0.33	0.33	0.18	0.14
Na_2O	2.49	3.04	3.76	0.74	2.59	3.06	0.60	0.14	1.10	0.68	0.04	0.00	0.02	0.03
K_2O	0.15	0.19	0.44	0.06	0.14	0.25	0.07	0.04	0.12	0.03	0.00	0.01	0.00	0.00
P_2O_5	0.06	0.08	0.07	0.08	0.06	0.08	0.05	0.00	0.00	0.00	0.00	0.01	0.00	0.00
LOI	0.57	0.77	1.37	3.99	1.98	1.65	2.92	2.37	3.34	1.12	10.55	11.54	2.69	3.87
S	0.03	0.02	0.02	0.01	0.01	0.01	0.01	0.00	0.02	0.01	0.01	0.02	0.02	0.14
Total	100.63	99.29	100.49	100.65	99.40	99.87	100.16	99.31	100.16	99.52	100.71	100.09	100.62	100.40
Ba	25	44	30	16	45	53	15	36	40	19	5	23	6	8
Cl	298	145	3347	382	192	393	160	109	85	70	101	309	97	115
Cr	199	191	180	267	310	214	377	130	171	119	1417	1783	2717	2733
Cu	89	215	27	132	69	28	70	25	74	27	2	6	34	8
Ga	17	15	14	14	14	15	10	19	11	10	3	2	2	0
Nb	6	4	3	6	6	6	7	4	3	3	0	0	1	0
Ni	70	69	65	81	156	101	88	87	81	63	2297	2285	1811	1830
Pb	5	6	1	7	6	0	5	1	2	2	0	0	2	0
Rb	5	7	7	3	5	7	3	3	4	2	2	2	2	2
Sr	120	183	153	21	102	144	50	141	180	166	2	1	1	1
Th	5	1	1	1	1	2	3	3	1	1	0	0	1	1
V	274	287	290	333	241	267	259	336	80	87	8	14	0	0
Y	22	26	25	23	24	27	21	5	4	4	1	1	1	2
Zn	73	64	40	95	69	66	71	93	38	36	43	44	46	42
Zr	41	55	43	50	49	48	40	5	8	6	8	9	8	8
La	0	2	2	0	0	0	0	0	2	0	2	3	0	2
Ce	0	0	3	0	0	0	0	0	0	0	0	0	0	0
Nd	0	22	20	0	1	2	4	4	2	0	6	4	0	6
Nb/Th	1.2	4	3	6	6	3	2.3	1.3	3	3				
Nb/Y	0.27	0.20	0.12	0.20	0.25	0.22	0.33	0.80	0.75	0.75				
Ti/V	20	15	18	16	20	21	17	3	8	7				

Table 1. (Continued)

Sample	BP-70	BP-51	BE-11	BE-4	BE-8	BP-62B	BP-74	BE-13	BP-45B	BP-65A	BP-52A	BP-57B	BE-9
Rock name	wehrlite	wehrlite	wehrlite	pyroxenite	pyroxenite	lherzolite	lherzolite	lherzolite	lherzolite	harzburgite	harzburgite	harzburgite	harzburgite
SiO_2	42.89	46.07	51.48	47.03	48.61	40.57	39.75	40.35	39.25	39.73	41.03	41.96	38.54
TiO_2	0.06	0.03	0.03	0.25	0.05	0.03	0.01	0.00	0.01	0.01	0.04	0.03	0.00
Al_2O_3	1.28	1.44	1.52	4.75	1.79	1.23	0.82	1.09	0.88	0.86	0.66	1.20	0.56
$Fe_2O_3^T$	12.85	7.62	7.90	11.04	7.63	8.66	8.53	8.83	9.77	9.24	8.99	9.18	8.46
MnO	0.21	0.15	0.15	0.18	0.13	0.12	0.12	0.14	0.14	0.13	0.13	0.12	0.12
MgO	29.54	36.12	35.54	20.25	25.31	39.14	41.24	37.81	40.05	42.58	42.28	37.38	40.04
CaO	9.90	0.99	1.60	16.22	16.03	0.61	0.88	0.69	1.09	0.61	0.90	0.94	0.57
Na_2O	0.07	0.05	0.04	0.27	0.08	0.08	0.04	0.07	0.03	0.05	0.02	0.08	0.05
K_2O	0.01	0.01	0.01	0.01	0.00	0.01	0.01	0.01	0.01	0.01	0.02	0.01	0.00
P_2O_5	0.00	0.00	0.00	0.00	0.00	0.00	0.00	0.00	0.00	0.01	0.00	0.00	0.00
LOI	3.86	7.42	2.44	0.49	1.11	10.25	9.19	11.88	8.42	8.81	6.58	9.97	10.91
S	0.01	0.01	0.01	0.02	0.01	0.01	0.01	0.02	0.02	0.02	0.01	0.01	0.01
Total	100.67	99.90	100.71	100.52	100.76	100.71	100.61	100.88	99.67	100.24	100.66	100.90	100.22
Ba	28	24	4	11	11	14	4	17	15	14	15	12	12
Cl	46	80	54	57	22	186	89	172	162	74	58	260	89
Cr	1562	5459	3948	786	3912	2145	1936	2099	2548	2199	1924	2373	2159
Cu	29	12	14	126	25	7	17	0	19	20	24	6	2
Ga	4	3	2	3	4	2	1	4	4	4	3	2	3
Nb	4	0	0	4	4	0	0	0	0	0	0	0	0
Ni	507	1030	897	247	584	2249	2157	2542	2195	2175	2417	2400	2075
Pb	12	0	3	3	0	0	0	0	2	0	0	1	0
Rb	4	2	3	2	2	5	1	3	3	2	1	2	2
Sr	4	3	3	16	7	6	1	9	4	3	1	3	1
Th	1	2	1	1	1	1	0	0	1	0	1	2	0
V	67	41	44	222	84	24	37	20	23	37	10	30	21
Y	3	3	4	10	4	3	1	1	2	2	3	3	2
Zn	59	44	43	41	36	45	43	44	51	48	47	44	42
Zr	7	8	8	9	8	8	8	8	9	8	8	8	8
La	5	0	0	0	0	0	5	1	0	2	0	2	2
Ce	0	0	0	0	0	0	0	0	0	0	0	0	0
Nd	3	1	0	3	14	6	8	0	5	0	4	2	3

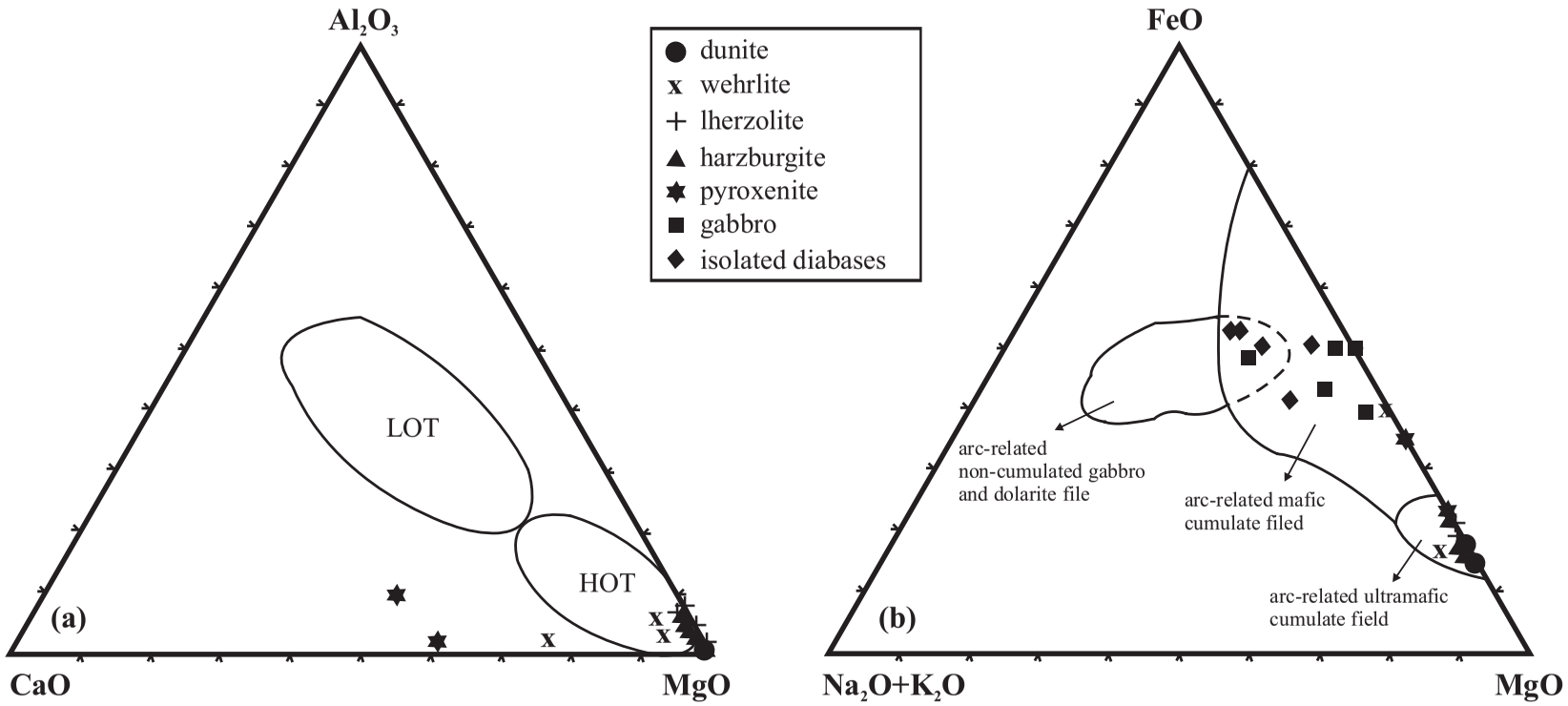

Figure 8. Major element contents of mafic-ultramafic cumulates from the Orhaneli ophiolite plotted on variation diagrams. (a) Al_2O_3-CaO-MgO diagram showing the compositions of ultramafic cumulates (Nicolas & Jackson 1972); (b) mafic-ultramafic cumulate samples plotted on an AFM diagram. Fields of cumulate and non-cumulate rocks are from Beard (1986). HOT– Harzburgite Ophiolite Type, LOT– Lherzolite Ophiolite Type.

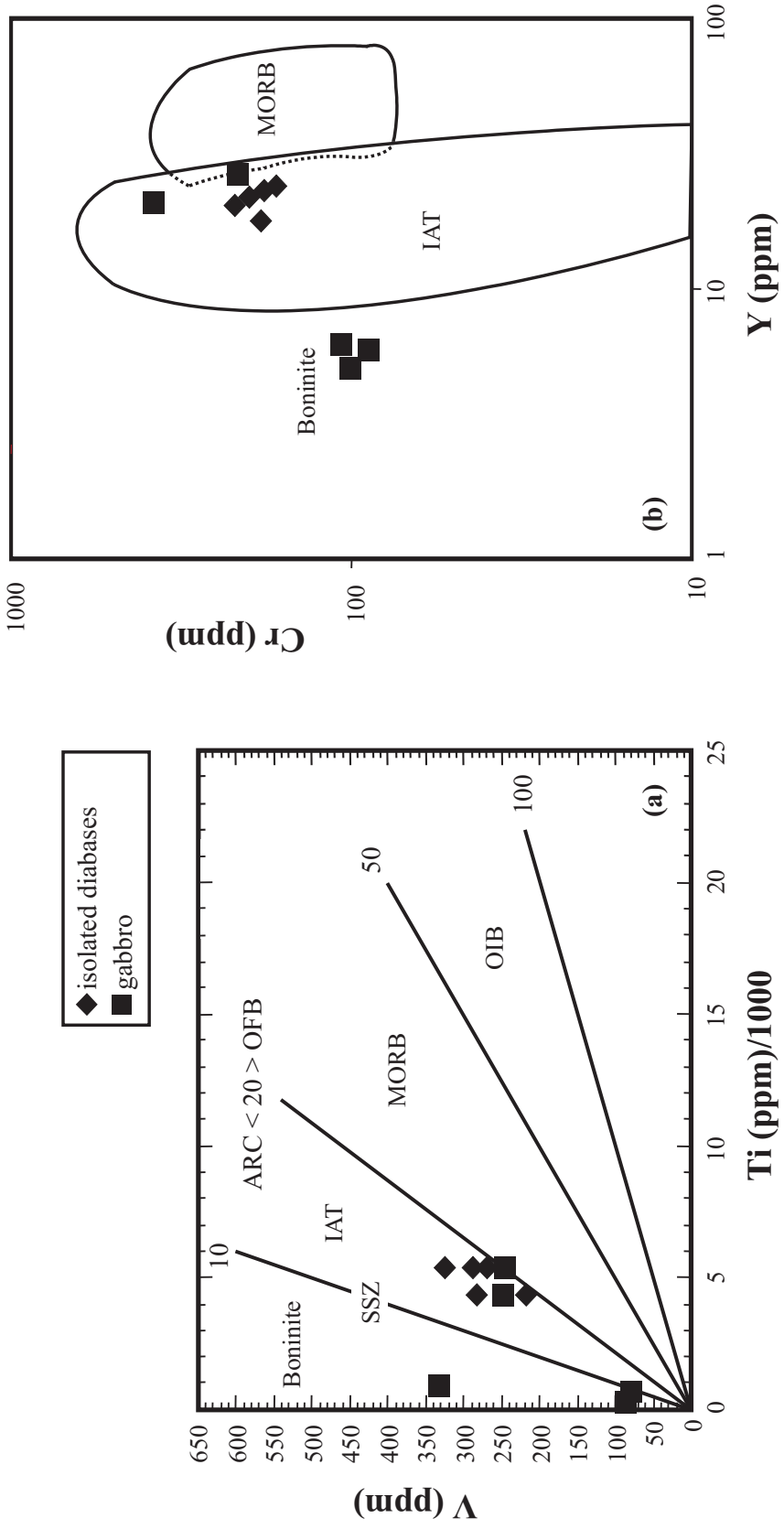

Figure 9. Trace element discrimination diagrams for the Orhaneli ophiolite: (a) Ti-V diagram (Shervais 1982); (b) Cr-Y diagram (Pearce 1982). IAT– island arc tholeiite; MORB– mid-ocean ridge basalt; SSZ– suprasubduction zone; OIB– ocean island basalt.

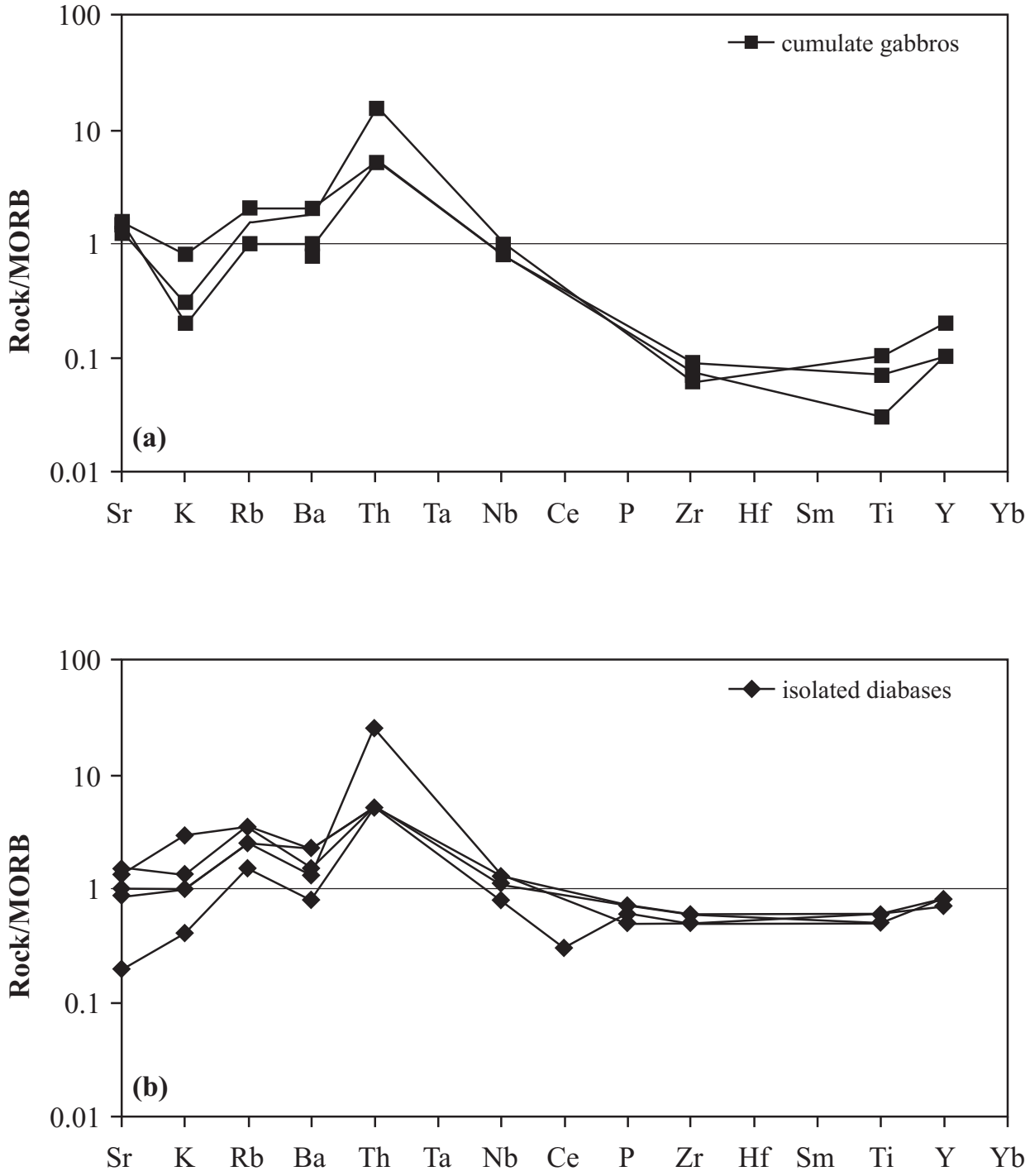

Figure 10. Tectonomagmatic discrimination diagrams for cumulate gabbros and isolated diabases of the Orhaneli ophiolite: (a) Nb/Th vs Y diagram (Jenner *et al.* 1991); (b) Ti-Zr diagram (Pearce & Cann 1973). The shaded field is from Johnson & Fryer (1990).

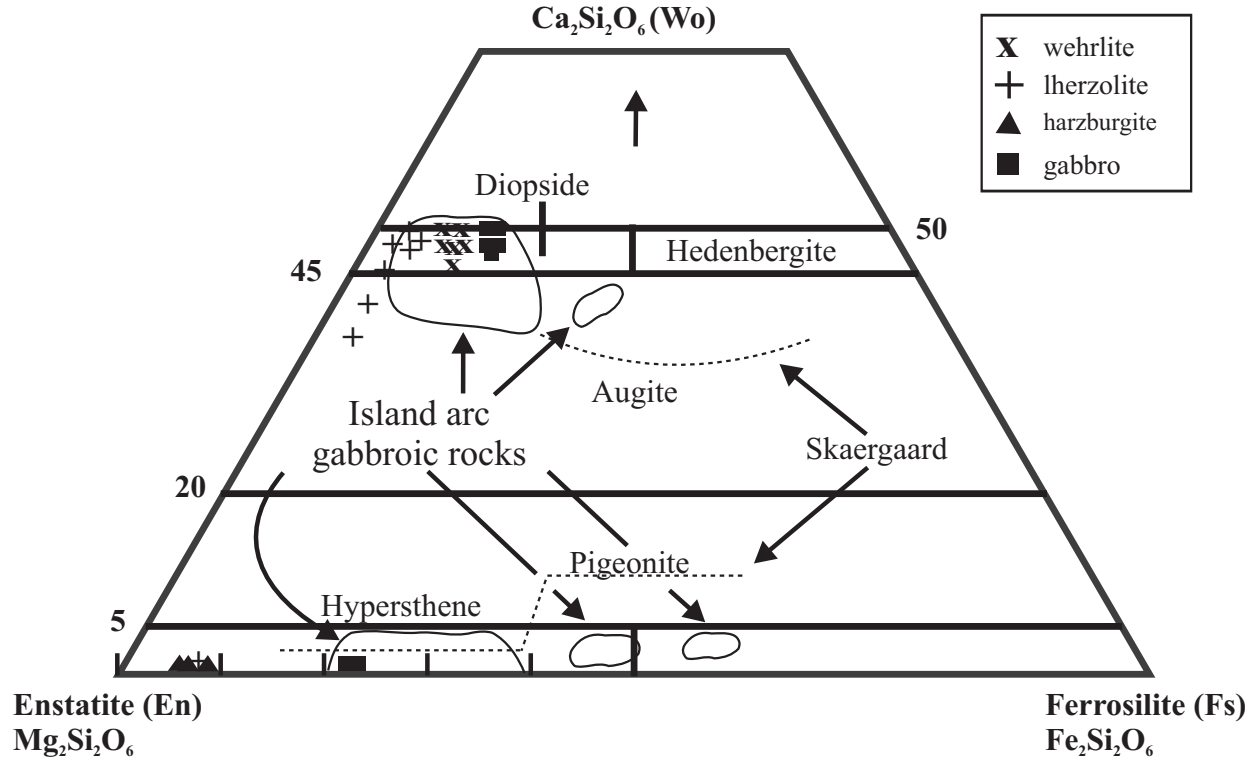

Figure 11. MORB–normalized spider diagrams for the cumulate gabbros (a) and isolated diabases (b) of the Orhaneli Ophiolite (normalizing values from Pearce 1983).

Table 2. The results of microprobe analyses of olivine crysts in peridotitic cumulates.

Lithology	WEHRLITE				HARZBURGITE					LHERZOLITE				
Sample	BP-70	BP-70	BP-70	BP-70	BP-65A	BP-65A	BP-65A	BP-52A	BP-52A	"04-87	"04-66	BP-45b	04-91A	"04-73
	OLV	OLV	OLV	OLV	OLV	OLV	OLV	OLV	OLV	OLV	OLV	OLV	OLV	OLV
SiO_2	39.54	39.47	39.31	39.60	41.05	41.00	41.64	40.85	40.93	39.37	40.32	40.38	40.55	40.75
Cr_2O_3	0.02	0.000	0.01	0.00	0.00	0.00	0.46	0.00	0.00	0.03	0.01	0.01	0.00	0.01
NiO	0.10	0.09	0.02	0.16	0.52	0.48	0.01	0.42	0.38	0.43	0.38	0.38	0.40	0.42
FeO	17.61	16.32	17.88	17.58	9.32	9.12	4.75	8.78	9.00	9.23	9.14	9.14	9.48	8.96
MnO	0.21	0.23	0.31	0.30	0.18	0.18	0.12	0.10	0.10	0.08	0.14	0.09	0.14	0.09
MgO	42.42	42.34	42.28	42.44	48.82	48.41	35.64	49.46	49.70	49.28	49.05	49.47	48.91	49.25
CaO	0.00	0.04	0.02	0.01	0.00	0.03	0.09	0.00	0.00	0.00	0.01	0.01	0.03	0.01
	99.92	98.80	99.86	100.12	99.89	99.25	83.50	99.62	100.12	98.41	99.05	99.48	99.52	99.52
formula calculated on the basis of 4 oxygens														
Si	1.005	1.010	1.002	1.005	1.006	1.010	1.180	1.001	0.999	0.982	0.997	0.994	0.999	1.001
Cr	0.000	0.000	0.000	0.000	0.000	0.000	0.010	0.000	0.000	0.001	0.000	0.000	0.000	0.000
Ni	0.002	0.002	0.000	0.003	0.010	0.010	0.000	0.008	0.008	0.009	0.008	0.008	0.008	0.008
Fe	0.375	0.356	0.381	0.373	0.191	0.188	0.113	0.180	0.184	0.192	0.189	0.188	0.195	0.184
Mn	0.005	0.005	0.007	0.006	0.004	0.004	0.003	0.002	0.002	0.002	0.003	0.002	0.003	0.002
Mg	1.607	1.615	1.606	1.606	1.783	1.778	1.506	1.807	1.808	1.832	1.807	1.814	1.795	1.803
Ca	0.000	0.001	0.001	0.000	0.000	0.001	0.003	0.000	0.000	0.000	0.000	0.000	0.001	0.000
Total	2.994	2.990	2.998	2.995	2.994	2.990	2.815	2.999	3.001	3.018	3.003	2.998	3.001	2.999
Fo	81.00	82.00	81.00	81.00	90	90	93	91	91	92	91	91	90	91

(Juteau *et al.* 1988), all of which are thought to have been formed in a suprasubduction zone tectonic environment.

Clinopyroxene

The clinopyroxene in the ultramafic cumulates (wehrlite, lherzolite) is diopside ($En_{45–57}Wo_{46–50}Fs_{3–6}$) with low Fe and high Mg (Tables 3 & 4). Especially in lherzolites, some clinopyroxenes are augite (Figure 12). The clinopyroxene Fe content increases from lherzolites to gabbros, even if by small amounts. The diopside composition in gabbroic cumulates is $En_{41–44}Wo_{48–50}Fs_{8–9}$. Taking the clinopyroxene composition as a base, the ultramafic cumulates and gabbroic cumulates of the Orhaneli ophiolites are conformable with the rocks formed in an island arc setting (Figure 12). The Mg# (Mg#= 100 × Mg / [Mg + Fe]) of the

Table 3. The results of microprobe analyses of clinoproxene crysts in cumulate lherzolite.

Lithology	LHERZOLITE						
Sample	"04-87	"04-87	"04-66	BP-45B	BP-45B	BP-45B	04-91A
	CPX	CPX	CPX	CPX	CPX	CPX	CPX
SiO_2	50.63	50.80	52.06	53.79	52.04	52.57	53.59
TiO_2	0.16	0.08	0.10	0.06	0.04	0.08	0.04
Al_2O_3	3.15	3.51	2.06	2.08	1.66	2.15	2.01
Cr_2O_3	0.87	1.08	0.95	0.86	0.71	0.97	0.55
FeO	2.02	2.21	2.25	3.16	3.03	2.07	1.93
NiO	0.03	0.06	0.01	0.03	0.03	0.01	0.08
MnO	0.11	0.04	0.00	0.07	0.09	0.04	0.09
MgO	16.48	16.46	17.81	20.60	19.16	16.95	17.34
CaO	24.13	23.44	23.18	18.80	21.23	23.99	23.87
Na_2O	0.16	0.23	0.12	0.10	0.12	0.13	0.17
	97.73	97.90	98.53	99.57	98.13	98.97	99.67
formula calculated on the basis of 6 oxygens							
Si	1.893	1.893	1.923	1.944	1.928	1.934	1.951
Al IV	0.107	0.107	0.077	0.056	0.072	0.066	0.049
Al VI	0.032	0.047	0.013	0.033	0.000	0.027	0.038
Ti	0.005	0.002	0.003	0.002	0.001	0.002	0.001
Cr	0.026	0.032	0.028	0.024	0.021	0.028	0.016
Ni	0.001	0.002	0.000	0.001	0.001	0.000	0.002
Fe	0.063	0.069	0.069	0.095	0.094	0.064	0.059
Mn	0.003	0.001	0.000	0.002	0.003	0.001	0.003
Mg	0.918	0.914	0.980	1.109	1.058	0.929	0.941
Ca	0.967	0.936	0.917	0.728	0.843	0.946	0.931
Na	0.012	0.017	0.009	0.007	0.009	0.009	0.012
Total	4.026	4.020	4.020	4.002	4.029	4.007	4.002
En	47.1	47.6	49.8	57.4	53.0	47.9	48.7
Fs	3.2	3.6	3.5	4.9	4.7	3.3	3.0
Wo	49.6	48.8	46.6	37.7	42.3	48.8	48.2
Mg# [100Mg/(Mg+Fe)]	93.57	92.98	93.42	92.10	91.84	93.55	94.10

Table 4. The results of microprobe analyses of clinoproxene crysts in mafic-ultramafic cumulates.

Lithology	WEHRLITE						GABBRO			GABBRONORITE				
Sample	BP-70	BP-70	BP-70	BP-70	BP-70	BP-70	BP-71	BP-71	BP-71	BP-73	BP-73	BP-73	BP-73	BP-73
	CPX	CPX	CPX	CPX	CPX	CPX	CPX	CPX	CPX	CPX	CPX	CPX	CPX	CPX
SiO_2	52.97	52.99	52.45	51.54	52.36	52.81	50.68	51.26	50.90	51.19	51.02	50.80	50.83	50.81
TiO_2	0.10	0.10	0.13	0.10	0.09	0.12	0.16	0.07	0.13	0.11	0.13	0.14	0.16	0.18
Al_2O_3	2.01	1.53	1.91	1.75	1.95	1.95	5.02	4.74	5.04	5.07	4.93	5.26	5.46	5.51
Cr_2O_3	0.42	0.32	0.45	0.36	0.36	0.41	0.03	0.03	0.03	0.00	0.02	0.00	0.00	0.01
FeO	3.88	3.50	3.57	4.18	3.84	3.69	4.94	5.03	5.01	5.05	5.33	5.11	5.23	5.21
MnO	0.08	0.14	0.09	0.10	0.09	0.12	0.15	0.15	0.10	0.17	0.09	0.07	0.11	0.16
MgO	16.21	16.50	16.14	16.87	16.20	16.19	14.55	14.76	14.57	14.61	14.62	14.28	14.13	14.06
CaO	24.13	24.61	24.30	22.70	24.16	24.66	22.38	22.40	23.66	22.41	22.84	23.25	23.28	23.22
Na_2O	0.13	0.11	0.16	0.10	0.16	0.11	0.19	0.19	0.20	0.19	0.23	0.24	0.19	0.22
	99.92	99.81	99.18	97.70	99.21	100.06	98.12	98.66	99.66	98.85	99.20	99.16	99.39	99.37
formula calculated on the basis of 6 oxygens														
Si	1.944	1.948	1.940	1.935	1.938	1.939	1.895	1.905	1.881	1.899	1.892	1.885	1.882	1.882
Al IV	0.056	0.052	0.060	0.065	0.062	0.061	0.105	0.095	0.119	0.101	0.108	0.115	0.118	0.118
Al VI	0.031	0.014	0.023	0.013	0.023	0.023	0.116	0.113	0.101	0.121	0.107	0.115	0.120	0.122
Ti	0.003	0.003	0.004	0.003	0.002	0.003	0.004	0.002	0.004	0.003	0.004	0.004	0.004	0.005
Cr	0.012	0.009	0.013	0.011	0.010	0.012	0.001	0.001	0.001	0.000	0.001	0.000	0.000	0.000
Fe	0.114	0.103	0.106	0.126	0.114	0.109	0.149	0.150	0.149	0.151	0.159	0.153	0.156	0.155
Mn	0.002	0.004	0.003	0.003	0.003	0.004	0.005	0.005	0.003	0.005	0.003	0.002	0.003	0.005
Mg	0.886	0.904	0.890	0.944	0.894	0.886	0.811	0.818	0.802	0.808	0.808	0.790	0.780	0.776
Ca	0.949	0.969	0.963	0.914	0.958	0.970	0.897	0.892	0.937	0.891	0.907	0.924	0.924	0.921
Na	0.009	0.008	0.011	0.007	0.012	0.008	0.013	0.013	0.014	0.014	0.016	0.017	0.014	0.016
Total	4.009	4.016	4.014	4.021	4.017	4.014	3.996	3.995	4.012	3.994	4.005	4.005	4.001	4.001
En	45.5	45.7	45.4	47.6	45.4	45.1	43.7	43.9	42.5	43.7	43.1	42.3	41.9	41.9
Fs	5.9	5.2	5.4	6.4	5.8	5.5	8.0	8.1	7.9	8.2	8.5	8.2	8.4	8.4
Wo	48.7	49.0	49.2	46.0	48.7	49.4	48.3	48.0	49.6	48.2	48.4	49.5	49.7	49.7
Mg/(Mg+Fe)	88.60	89.77	89.35	88.22	88.69	89	84	85	84	84	84	84	83	83

clinopyroxene ranges from 91 to 94 in lherzolite (Table 3), from 88 to 90 in wehrlite, and from 83 to 85 in gabbroic rocks (Table 3) showing that the mafic-ultramafic cumulates of the Orhaneli ophiolite have clinopyroxenes with Mg-numbers as high as in other Eastern Mediterranean ophiolites.

The Cr_2O_3 content of the clinopyroxene in mafic-ultramafic cumulates of the Orhaneli ophiolite (Tables 3 & 4) shows a gradual decrease with decreasing Mg# from lherzolite (Cr_2O_3 in clinopyroxene= 0.6–1.1%) to wehrlite (Cr_2O_3 in clinopyroxene= 0.3–0.5%) and gabbroic cumulates (Cr_2O_3 in clinopyroxene= 0.01–0.03%). The gradual decrease of Cr may be related with the gradual depletion of Cr during the differentiation of the basic magma to produce the ultramafic rocks first and then the mafic rocks (Hodges & Papike 1976).

Clinopyroxenes in cumulates are characterized by low TiO_2 contents averaging 0.1wt%. It is proposed that the low Ti ophiolites formed from a variably depleted source in a suprasubduction tectonomagmatic regime, similar to the Vourinos (Beccaluva *et al.* 1984), Troodos (Cameron 1985) and Oman (Pallister & Hopson 1981) ophiolites, which display an island arc tholeiitic and/or boninitic affinity.

Orthopyroxene

With internal differentiation, lherzolites and harzburgites grade into dunite, which forms the basement of the ultramafic cumulate sequence. In both the harzburgites and lherzolites the orthopyroxenes are enstatites (En_{90-92}) with high Mg content (Table 5). The orthopyroxenes in the

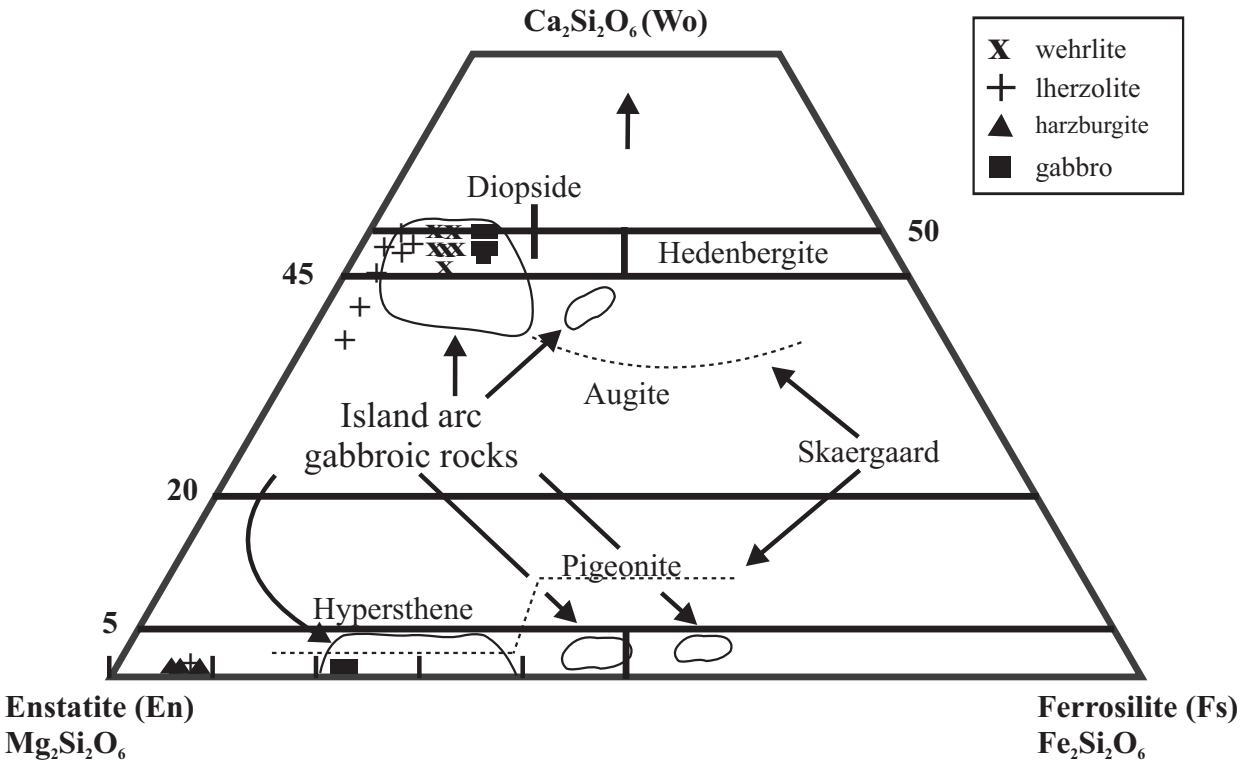

Figure 12. Chemical composition of clinopyroxenes (cpx) and orthopyroxenes (opx) from mafic-ultramafic cumulates in the pyroxene ternary diagram of Walker *et al.* (1973). Island arc fields from Beard (1986).

Table 5. The results of microprobe analyses of orthopyroxene crysts in peridotitic cumulates.

Lithology	HARZBURGITE					LHERZOLITE				
Sample	BP-65A	BP-65A	BP-65A	BP-52A	BP-52A	"04-87	"04-66	"04-66	04-91A	"04-73
	OPX	OPX	OPX	OPX	OPX	OPX	OPX	OPX	OPX	OPX
SiO_2	57.67	57.29	57.09	57.76	57.67	55.38	56.22	55.76	56.10	56.84
TiO_2	0.01	0.03	0.02	0.00	0.01	0.06	0.03	0.05	0.01	0.03
Al_2O_3	0.82	1.11	1.29	0.83	0.83	1.99	1.55	1.75	1.99	1.62
Cr_2O_3	0.30	0.35	0.42	0.38	0.36	0.42	0.31	0.52	0.41	0.39
NiO	0.11	0.04	0.05	0.13	0.08	0.03	0.06	0.08	0.11	0.07
FeO	6.38	6.26	6.27	5.92	5.65	6.17	6.17	5.51	5.96	6.14
MnO	0.15	0.05	0.19	0.16	0.13	0.09	0.08	0.04	0.16	0.14
MgO	33.95	33.97	33.54	34.65	34.42	34.05	34.18	34.01	33.64	34.44
CaO	0.22	0.55	0.88	0.47	1.06	0.39	0.54	0.63	0.57	0.29
	99.61	99.66	99.76	100.29	100.22	98.58	99.15	98.37	98.95	99.94
formula calculated on the basis of 6 oxygens										
Si	1.994	1.981	1.976	1.983	1.982	1.940	1.957	1.952	1.955	1.960
Ti	0.000	0.001	0.000	0.000	0.000	0.001	0.001	0.001	0.000	0.001
Al	0.033	0.045	0.053	0.034	0.033	0.082	0.063	0.072	0.082	0.066
Cr	0.008	0.010	0.012	0.010	0.010	0.012	0.009	0.014	0.011	0.011
Ni	0.003	0.001	0.001	0.004	0.002	0.001	0.002	0.002	0.003	0.002
Fe	0.184	0.181	0.181	0.170	0.162	0.181	0.180	0.161	0.174	0.177
Mn	0.004	0.001	0.006	0.005	0.004	0.003	0.002	0.001	0.005	0.004
Mg	1.749	1.750	1.730	1.773	1.763	1.778	1.773	1.775	1.747	1.770
Ca	0.008	0.020	0.033	0.017	0.039	0.015	0.020	0.024	0.021	0.011
Total	3.985	3.991	3.991	3.995	3.996	4.012	4.006	4.003	3.998	4.001
En	90	91	91	91	92	91	91	92	91	91

ultramafic cumulates contain low Al_2O_3 (<2%). Dick (1977) also noted that ultramafic cumulates include cumulus orthopyroxenes containing low Al_2O_3 (<2%) compared to those in tectonic ultramafics.

Orthopyroxene compositions in the cumulate gabbronorites interlayered with the ultramafic cumulates of the Orhaneli Ophiolite are hypersthene ($En_{76–77}Wo_{1–2}Fs_{21–22}$); Mg# varies between 77 and 78 (Table 6). Thus the chemical composition of the orthopyroxenes is similar to that of the orthopyroxenes present in the cumulate gabbroic rocks in other suprasubduction zone ophiolites (Figure 12). The depletion of Cr_2O_3 (≤0.04%) in the orthopyroxenes in the cumulate gabbronorites compared to the ultramafic cumulates containing orthopyroxenes with 0.3–0.5 wt% Cr_2O_3 is linked to fractionation in the parent liquid.

Plagioclase

Plagioclase is a major constituent in gabbroic cumulates from the Orhaneli ophiolite. It occurs as a cumulus phase in both the layered gabbro cumulates and gabbronorites. The An content ranges from $An_{86.3–98.8}$ in the gabbroic rocks (Table 7), and this high An content and the limited compositional range in the gabbroic cumulates from the Orhaneli ophiolite are consistent with SSZ-type ophiolites and comparable with the gabbros in the Eastern Mediterranean ophiolites (Figure 13). Thus calcic plagioclases in the Orhaneli gabbroic cumulates have high CaO/Na_2O ratio and are probably derived from a CaO-rich liquid (Panjasawatwong *et al.* 1997).

Spinel

Chromite, which belongs to the spinel group of minerals, occurs as scattered accessory minerals in the cumulate peridotites of the Orhaneli ophiolites or forms massive ore bodies concentrated as layers in cumulate dunites. Since the Cr-spinels form a very stable crystallochemical phase in serpentinized peridotites, they are used as petrogenetical indicators (Irvine 1967; Dick & Bullen 1984).

Thayer (1960) differentiated the podiform chromites in the ophiolite complexes as high-Cr chromite (metallurgic, Cr_2O_3 > 40 wt%) and as high-Al chromite (refractory, Al_2O_3 > 25 wt%). Zhou & Robinson (1994) stated that the chromites with these chemical compositions have affinities with boninitic and MORB-like tholeiitic magmas, respectively. The chemistry of the Cr-spinels (Cr_2O_3= 40–55 wt%) observed in the peridotitic cumulates grading from dunites to pyroxene-bearing peridotites in the study area display a narrow compositional range. The Al_2O_3 content of the chromites analyzed from the ultramafic cumulates is less than 25 wt%, except in two analyses (Tables 8 & 9). The TiO_2 content of Cr-spinel in the ultramafic cumulates is very low (<0.1 wt%). A TiO_2-Al_2O_3 diagram shows that Cr-spinel compositions from the Orhaneli ophiolite are consistent with formation in a suprasubduction zone environment (Figure 14).

Cr# (=Cr / [Cr+Al]) is high in harzburgites and ranges from 0.65 to 0.73 (Table 8); it is lower in lherzolites with an average value of 0.50 (Table 9). In the Cr#–Mg# (= Mg / [Mg+Fe^{2+}]) diagram, the Cr-spinels present in the ultramafic cumulates of the Orhaneli ophiolite fall in the SSZ-type ophiolite field (Figure 15). It was claimed that the high Cr# and low-Ti chromites in the Marmaris (Muğla) peridotites of the Eastern Mediterranean Ophiolite Belt are products of boninitic magma in a suprasubduction setting (Uysal *et al.* 2005). Chromites of the Pozantı-Karsantı (Adana), Mersin and Kızıldağ (Hatay) ophiolites are likewise reported to have a high Cr_2O_3 percentage (>45 wt%) and these ophiolites are also thought to have formed in a suprasubduction zone environment (Anıl 1990; Bağcı *et al.* 2005; Parlak *et al.* 1996, 2002).

Discussion and Conclusion

The Orhaneli ophiolite, situated in the western İzmir-Ankara-Erzincan Suture Zone (İAESZ) south of Bursa, preserves the mantle-crust transition zone. The Harmancık ophiolite, south of the Orhaneli ophiolite, is formed almost entirely of mantle tectonites.

The mantle-crust transition zone, marking the petrological MOHO, is characterized by layered cumulate sequence and layered cumulate gabbros between upper mantle peridotites and lower crustal gabbros (Greenbaum 1972). The Orhaneli ophiolite consists mostly of magmatic layering of the ultramafic cumulates and very rare layered gabbroic cumulates, locally cross-cut by isolated diabase dykes.

Field observations show that the mafic-ultramafic cumulates of the Orhaneli ophiolite have basal cumulate dunites exposed in the eastern part of the investigated area. Numerous centimetre to metre-thick chromitite bands can be traced within cumulate dunites, which are interlayered with wehrlites that locally exhibit internal

Table 6. The results of microprobe analyses of orthopyroxene crysts in cumulate gabbroic rocks.

Lithology	GABBRONORITE							
Sample	BP-73	BP-73	BP-73	BP-73	BP-73	BP-73	BP-73	BP-73
	OPX	OPX	OPX	OPX	OPX	OPX	OPX	OPX
SiO_2	52.92	52.73	52.77	52.91	52.67	52.83	52.80	52.80
TiO_2	0.02	0.02	0.00	0.03	0.06	0.06	0.05	0.01
Al_2O_3	5.05	5.07	4.91	4.98	5.30	5.07	4.75	5.00
Cr_2O_3	0.01	0.02	0.04	0.01	0.01	0.01	0.00	0.02
MnO	0.23	0.30	0.29	0.33	0.28	0.23	0.31	0.28
CaO	0.44	0.43	0.41	0.46	0.37	0.45	0.40	0.73
MgO	27.27	27.32	27.33	27.10	27.47	27.27	27.50	27.04
FeO	14.27	14.14	14.21	13.85	13.91	13.88	13.92	14.19
	100.21	100.06	99.98	99.68	100.10	99.81	99.75	100.15
formulas on the basis of 6 oxygens								
Si	1.889	1.886	1.889	1.896	1.881	1.891	1.893	1.889
Ti	0.001	0.001	0.000	0.001	0.001	0.002	0.001	0.000
Al	0.213	0.214	0.207	0.210	0.223	0.214	0.201	0.211
Cr	0.000	0.001	0.001	0.000	0.000	0.000	0.000	0.001
Mn	0.007	0.009	0.009	0.010	0.009	0.007	0.009	0.008
Ca	0.017	0.017	0.016	0.018	0.014	0.017	0.015	0.028
Mg	1.451	1.456	1.458	1.447	1.462	1.454	1.469	1.442
Fe	0.426	0.423	0.426	0.415	0.415	0.416	0.417	0.425
Total	4.004	4.006	4.006	3.998	4.006	4.001	4.006	4.005
En	77.6	76.8	76.7	77.0	77.4	77.1	77.3	76.1
Fs	22.5	22.3	22.4	22.0	21.9	22.0	21.9	22.4
Wo	0.9	0.9	0.9	1.0	0.7	0.9	0.8	1.5
Mg#								
[100Mg/(Mg+Fe)]	77	77	77	78	78	78	78	77

Table 7. The results of microprobe analyses of plagioclase crysts in cumulate gabbroic rocks.

Lithology	GABBRONORITE					GABBRO		
Sample	BP-73	BP-73	BP-73	BP-73	BP-73	BP-71	BP-71	BP-71
	PLAG	PLAG	PLAG	PLAG	PLAG	PLAG	PLAG	PLAG
SiO_2	42.78	43.27	43.30	43.58	43.66	42.672	44.031	41.534
Al_2O_3	35.27	36.25	35.40	35.47	34.91	36.566	35.056	36.568
FeO	2.38	1.08	0.95	0.99	1.06	0.974	0.844	0.953
MnO								
MgO	1.92	0.75	0.82	0.74	1.33	0.894	0.648	0.856
CaO	15.04	16.36	18.17	17.55	17.00	19.457	18.247	19.281
Na_2O	1.30	0.94	0.61	0.87	1.08	0.187	0.937	0.105
K_2O	0.04	0.01	0.03	0.05	0.10	0.000	0.000	0.047
	98.75	98.74	99.32	99.29	99.17	100.84	99.796	99.378
formula on the basis of 6 oxygens								
Si	1.999	2.018	2.018	2.028	2.034	1.967	2.042	1.943
Al	1.943	1.992	1.944	1.946	1.917	1.986	1.916	2.017
Fe^{+3}	0.093	0.042	0.037	0.039	0.041	0.038	0.033	0.037
Total IV	4.036	4.052	3.999	4.013	3.993	3.991	3.990	3.997
Mg	0.134	0.052	0.057	0.051	0.093	0.061	0.045	0.060
Ca	0.753	0.817	0.907	0.875	0.849	0.961	0.907	0.967
Na	0.118	0.085	0.055	0.078	0.097	0.017	0.084	0.010
K	0.002	0.000	0.002	0.003	0.006	0.000	0.000	0.003
Total	5.042	5.008	5.020	5.020	5.038	5.030	5.026	5.036
Or	0.28	0.03	0.18	0.31	0.64	0.00	0.00	0.28
Ab	13.46	9.43	5.67	8.18	1.23	1.71	8.50	0.97
An	86.26	90.53	94.14	91.51	89.14	98.29	91.50	98.75

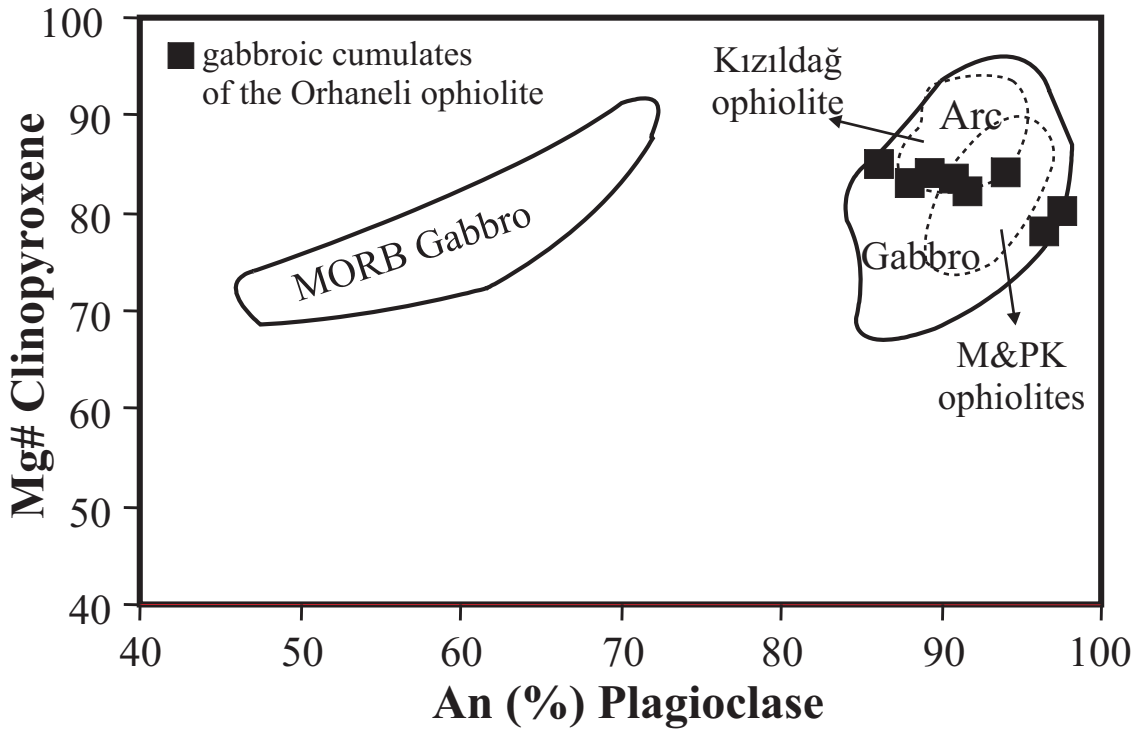

Figure 13. Composition of coexisting plagioclase (An-content) and clinopyroxene (Mg#) in the gabbroic cumulates. Fields of MORB and arc gabbros are from Burns (1985). Compositional ranges for the Kızıldağ ophiolite (Bağcı *et al.* 2005) and the Mersin and Pozantı-Karsantı (M & PK) ophiolites (Parlak *et al.* 1996; 2002) are shown as dashed lines.

layering between olivine- and clinopyroxene-rich layers. The clinopyroxene-rich levels sometimes constitute pyroxenites. The ultramafic cumulate levels also developed locally as interbedded peridotites including dunites grading into ortho- and/or clino-pyroxene-bearing peridotites such as wehrlite, lherzolite or harzburgite. The ultramafic cumulates are interlayered with the thin-layered gabbroic cumulates in three places, Osmaniye Village, Bursa-Orhaneli Road and Çınarcık Village (Figure 4). This cyclic layering suggests that there were several major replenishment pulses during formation of the cumulate suite crystallizing on the floor of a steady-state magma chamber. According to Ishiwatari (1994), distribution of Phanerozoic ophiolites shows two peaks, Ordovician and Jurassic–Cretaceous. The layered series is composed of interlayered gabbro and peridotite cumulates equivalent to oceanic layer 3 in the Cretaceous Semail (Oman) ophiolite and is thought to have been formed from a long-lived, elongated and periodically replenished magma chamber (Pallister & Hopson 1981; Juteau *et al.* 1988). The interlayered mafic and ultramafic cumulates overlying harzburgite tectonites in the Jurassic Vourinos ophiolite and the Ordovician Bay of Islands ophiolite are interpreted as the products of cumulate recycling (Jackson *et al.* 1975; Bedard 1991). However, in the SSZ Mesozoic Koryak Ophiolite Complex in the northwestern Pasific margin (Ishiwatari *et al.* 2003) the southern half of the complex consists mostly of depleted harzburgite, whereas the northern half is composed of ultramafic cumulates like the Harmancık Ophiolite and the Orhaneli Ophiolite.

In the petrographical studies, two crystallization orders were observed in the mafic-ultramafic cumulates, with adcumulate and mesocumulate textures in the Orhaneli ophiolite. One of them is ol-cpx-plag, occurring in the interbedded peridotitic (dunite, wehrlite, pyroxenite) and gabbroic cumulates in the eastern part of the Orhaneli ophiolite. The other order is olivine-clinopyroxene-orthopyroxene-plagioclase, seen in the dunites grading to wehrlites and two pyroxene peridotites (mostly lherzolites showing a transitional boundary with harzburgites, pyroxenite in places), and layered gabbroic rocks that are especially found in the western part of the Orhaneli

Table 8. The results of microprobe analyses of Cr-spinel crysts in cumulate harzburgite.

Lithology	HARZBURGITE									
Sample	BP-65A	BP-65A	BP-65A	BP-52A	BP-52A	BP-65A	BP-65A	BP-65A	BP-52A	BP-52A
	SP	SP	SP	SP	SP	SP	SP	SP	SP	SP
SiO_2	0.01	0.01	0.04	0.03	0.03	0.00	0.03	0.03	0.02	0.02
TiO_2	0.10	0.07	0.05	0.11	0.07	0.05	0.04	0.05	0.08	0.08
Al_2O_3	16.03	17.33	17.22	13.09	17.46	17.39	13.59	13.54	13.97	13.91
Cr_2O_3	48.40	47.45	47.67	51.18	47.42	47.75	54.85	54.80	54.48	54.66
FeO total	24.28	24.04	23.76	26.49	23.78	23.84	20.57	20.64	20.56	20.54
NiO	0.06	0.05	0.05	0.00	0.04	0.10	0.08	0.08	0.04	0.07
MnO	0.00	0.00	0.00	0.00	0.00	0.00	0.00	0.00	0.00	0.00
MgO	8.39	8.59	9.02	5.79	9.04	9.13	9.23	9.18	9.37	9.42
Total	97.28	97.53	97.81	96.70	97.84	98.28	98.39	98.35	98.52	98.72
FeO*	21.00	20.96	20.40	24.41	20.44	20.30	19.60	19.67	19.47	19.49
Fe_2O_3*	3.64	3.43	3.73	2.31	3.71	3.93	1.07	1.09	1.21	1.16
new TOTAL	97.63	97.87	98.18	96.91	98.21	98.64	98.50	98.43	98.57	98.82
* calculated on the basis of 32 oxygens for 24 cations										
formula calculated on the basis of 24 cations with estimated Fe^{2+} and Fe^{3+}										
Si	0.002	0.002	0.009	0.008	0.007	0.000	0.008	0.008	0.006	0.005
Ti	0.020	0.013	0.010	0.022	0.014	0.009	0.007	0.010	0.002	0.017
Al	5.034	5.390	5.330	4.267	5.395	5.352	4.250	4.240	4.354	4.325
Cr	10.192	9.899	9.893	11.190	9.829	9.858	11.504	11.505	11.390	11.401
Fe^{3+}	0.730	0.681	0.737	0.481	0.733	0.772	0.214	0.217	0.242	0.230
sum	15.978	15.985	15.980	15.969	15.978	15.991	15.984	15.981	15.993	15.978
Fe^{2+}	4.679	4.625	4.480	5.645	4.482	4.434	4.349	4.368	4.305	4.301
Ni	0.012	0.011	0.011	0.000	0.008	0.020	0.017	0.017	0.008	0.015
Mn	0.000	0.000	0.000	0.000	0.000	0.000	0.000	0.000	0.000	0.000
Mg	3.331	3.379	3.529	2.386	3.532	3.555	3.650	3.634	3.694	3.706
sum	8.022	8.015	8.020	8.031	8.022	8.009	8.016	8.019	8.007	8.022
Total	24.000	24.000	24.000	24.000	24.000	24.000	24.000	24.000	24.000	24.000
Cr# [Cr/(Cr+Al)]	0.67	0.65	0.65	0.72	0.65	0.65	0.73	0.73	0.71	0.72
Mg# [Mg/(Mg+Fe^{2+})]	0.42	0.42	0.44	0.30	0.44	0.44	0.46	0.45	0.46	0.46

ophiolite. In the same way, the ultramafic-mafic cumulates in the Neotethyan Semail Ophiolite are represented within two suites by Umino *et al.* (1990): a clinopyroxene series of dunite, wehrlite, and gabbro-diorite and a orthopyroxene series of lherzolite and gabbronorites. It was concluded there that both suites are related to subduction zone magmatism. Pearce (2003) stated the cumulate sequences of the very low Ti ophiolites (subduction-related) comprised dunite, peridotite with two pyroxenes in varying proportion and gabbros indicating possibly boninitic original magmas, whereas mafic-ultramafic cumulates in low Ti ophiolites (subduction-related) comprising dunite, wehrlite and gabbro may originate from island- arc tholeiitic magmas. By contrast the lower crustal units of MORB-type ophiolites are composed of dunite, troctolite and gabbro.

Petrochemical data reveal that the mafic-ultramafic cumulates and isolated diabase dykes of the Orhaneli ophiolite are compositionally similar to arc-related magmas. The multi-element patterns of cumulate gabbros and isolated diabases show Th enrichment within the LILE group and the depletion of HFSE relative to MORB

Table 9. The results of microprobe analyses of Cr-spinel crysts in cumulate lherzolite.

Lithology	LHERZOLITE									
Sample	"04-66	"04-66	"04-66	BP-45B	04-91A	04-91A	"04-73	"04-73	"04-73	"04-73
	SP	SP	SP	SP	SP	SP	SP	SP	SP	SP
SiO_2	0.02	0.05	0.02	0.02	0.00	0.02	0.03	0.00	0.01	0.04
TiO_2	0.10	0.14	0.11	0.10	0.08	0.05	0.04	0.07	0.07	0.08
Al_2O_3	23.16	24.53	24.56	23.74	33.00	32.89	24.31	23.10	22.90	24.04
Cr_2O_3	45.56	43.98	43.77	43.16	34.84	34.84	41.19	43.01	43.15	43.00
FeO total	17.66	18.96	18.91	20.30	18.29	17.97	20.70	20.52	21.34	20.67
NiO	0.17	0.14	0.08	0.13	0.15	0.10	0.10	0.09	0.09	0.01
MnO	0.00	0.00	0.00	0.00	0.00	0.00	0.00	0.00	0.00	0.00
MgO	13.11	12.14	12.19	11.42	13.48	13.87	11.27	11.34	10.87	11.34
Total	99.79	99.95	99.65	98.88	99.87	99.27	97.84	98.16	98.45	99.20
FeO*	15.60	17.43	17.27	18.01	16.56	16.14	17.93	17.80	18.60	18.41
Fe_2O_3*	2.29	1.71	1.82	2.54	1.93	2.03	3.08	3.02	3.05	2.51
new TOTAL	100.01	100.09	99.82	99.11	100.03	99.47	97.94	98.43	98.73	99.42
* calculated on the basis of 32 oxygens for 24 cations										
formula calculated on the basis of 24 cations with estimated Fe^{2+} and Fe^{3+}										
Si	0.006	0.012	0.005	0.004	0.000	0.004	0.007	0.000	0.002	0.010
Ti	0.018	0.025	0.020	0.018	0.013	0.008	0.008	0.014	0.013	0.014
Al	6.695	7.088	7.112	6.974	9.151	9.648	7.204	6.848	6.800	7.038
Cr	8.834	8.524	8.501	8.504	6.481	5.970	8.186	8.552	8.592	8.444
Fe^{3+}	0.423	0.315	0.336	0.477	0.341	0.358	0.582	0.572	0.579	0.469
sum	15.976	15.964	15.975	15.978	15.987	15.988	15.986	15.986	15.986	15.975
Fe^{2+}	3.199	3.573	3.548	3.755	3.258	3.158	3.770	3.745	3.917	3.825
Ni	0.033	0.027	0.016	0.027	0.029	0.019	0.021	0.018	0.018	0.002
Mn	0.000	0.000	0.000	0.000	0.000	0.000	0.000	0.000	0.000	0.000
Mg	4.792	4.436	4.462	4.241	4.726	4.835	4.224	4.252	4.079	4.198
sum	8.024	8.036	8.025	8.022	8.013	8.012	8.014	8.014	8.014	8.025
Total	24.000	24.000	24.000	24.000	24.000	24.000	24.000	24.000	24.000	24.000
Cr/(Cr+Al)	0.55	0.54	0.53	0.53	0.41	0.37	0.53	0.56	0.56	0.55
Mg/(Mg+Fe^{2+})	0.60	0.55	0.56	0.53	0.60	0.60	0.53	0.53	0.51	0.52

indicating the characteristics of island arc tholeiites formed in a suprasubduction zone setting. The tectonomagmatic discrimination diagrams based on immobile trace elements (V, Ti, Nb, Y, Cr, Zr) suggest that cumulate gabbros were derived from IAT to possibly boninitic magmas whereas the isolated diabases have a clear IAT-affinity. Boninites, generally considered to be a product of subduction-zone related melting, are encountered solely in the forearc region of modern intraoceanic subduction zone setting (Hawkins *et al.* 1984). Stern & Bloomer (1992) suggested that low Ti (<1 wt%; island- arc tholeiite) and very low Ti (<0.4 wt%; boninite-like) ophiolite formed in an early arc setting. These insights obtained from field and petrochemical studies of the Orhaneli ophiolite indicate that it was probably formed in the forearc region, in a suprasubduction zone tectonic setting within the northern branch of the Neotethyan Ocean. Moreover, the composition of olivine (Fo_{81-93}), clinopyroxene ($Mg\#_{83-94}$), orthopyroxene ($Mg\#_{77-92}$), plagioclase (An_{86-99}) and Cr-spinel ($Cr\#_{0.40-0.73}$) in the mafic-ultramafic cumulates of the Orhaneli ophiolite denote a clear suprasubduction zone signature.

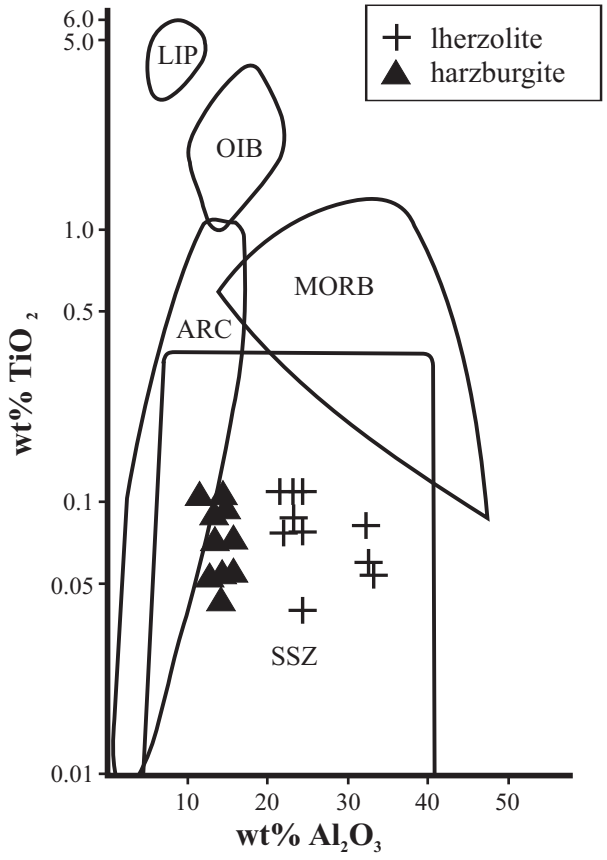

Figure 14. TiO_2-Al_2O_3 diagram showing the compositions of Cr-spinels of the ultramafic cumulates in the Orhaneli ophiolite. Fields from Kamenetsky *et al.* (2001).

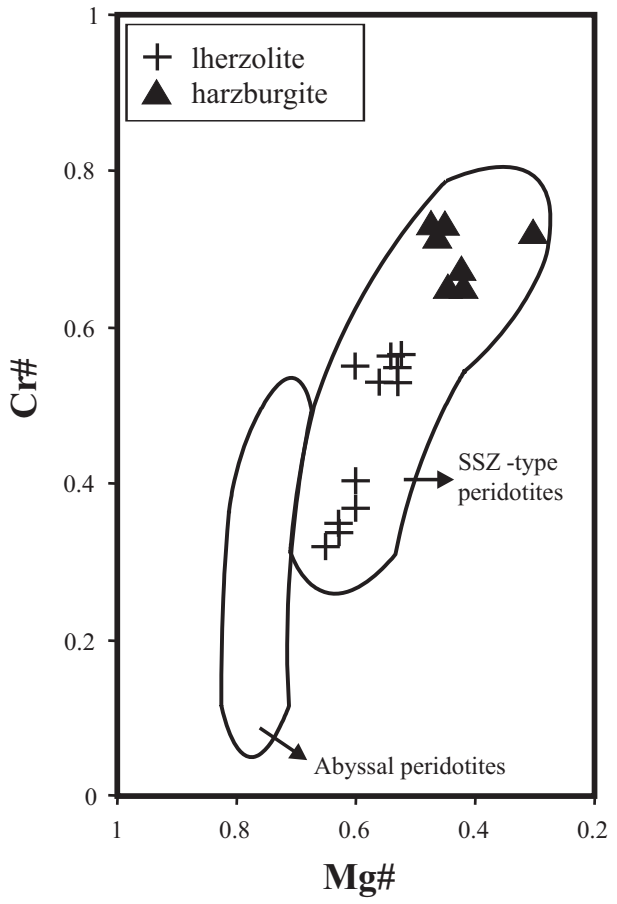

Figure 15. Cr# vs Mg# diagram showing the compositions of Cr-spinels of the ultramafic cumulates in the Orhaneli ophiolite. Fields from Dick & Bullen (1984).

The Jurassic Ligurian, Mirdita, Pindos and Vourinos Ophiolites in the Alps, Apennines and Dinarides-Hellenides, and the Cretaceous Mediterranean ophiolites (Troodos, Lycian, Pozantı-Karsantı, Mersin, Kızıldağ, Neyriz, Semail and Muslim Bagh) in the Troodos, Tauride, Zagros-Oman mountains and Himalayas show a MORB-affinity, with both MORB- and SSZ-like compositions and IAT-affinity progressively younging eastwards in age (Dilek & Flower 2003). The Cretaceous Orhaneli Ophiolite, thrust onto the İAESZ in northwestern Turkey, is considered to have been formed in a suprasubduction zone setting, probably in a forearc region, similar to that of other ophiolites in the Eastern Mediterranean area.

Acknowledgements

This study formed part of 'The investigation of ophiolite-related ore deposits, Project No: 16B15' of the General Directorate of the MTA. ES thanks TÜBİTAK for the scholarship (2005-NATO-B2) granted for geochemical studies in Keele University, England. David Emley (Keele University) is thanked for his analytical assistance. Thanks are due to Ursula Robert (Pierre and Marie Curie University, Paris) for helping provide related microprobe analyses. The authors are grateful to Martin F.J. Flower and Osman Parlak for their constructive comments, which considerably improved the paper. We also thank Nilgün Güleç and Durmuş Boztuğ for editorial comments.

References

ANIL, M. 1990. Pozantı-Karsantı, Mersin ve Kızıldağ (Hatay) ofiyolitlerindeki bazı kromit yataklarının morfolojik, yapısal ve jenetik özellikleri ile Akdeniz Bölgesindeki benzer kromit yataklarıyla karşılaştırılması [Character morpho-structural and genetic of some chromite deposits of the Pozantı-Karsantı, Mersin and Kızıldağ (Hatay) ophiolitic massifs and comparison with other Mediterranean chromite deposits]. *Doğa* [*Journal of Engineering and Environmental Sciences]* **14**, 645–675.

BACAK, G. & UZ, B. 2003. Dağardı güneyi (Kütahya) ofiyolitinin jeolojisi ve jeokimyasal özellikleri [The geology and geochemical characteristics of the Dağardı (Kütahya) ophiolite]. *Bulletin of İstanbul Technical University* **2**, 86–98 [in Turkish with English abstract].

BAĞCI, U., PARLAK, O. & HÖCK, V. 2005. Whole-rock and mineral chemistry of cumulates from the Kızıldağ (Hatay) ophiolite (Turkey): clues for multiple magma generation during crustal accretion in the southern Neotethyan ocean. *Mineralogical Magazine* **69**, 53–76.

BEARD, J.S. 1986. Characteristic mineralogy of arc-related cumulate gabbros: implications for the tectonic setting of gabbroic plutons and for andesite genesis. *Geology* **14**, 848–851.

BECCALUVA, L., OHNENSTETTER, D., OHNENSTETTER, M. & PAUPY, A. 1984. Two magmatic series with island arc affinities within the Vourinos ophiolite. *Contributions to Mineralogy and Petrology* **85**, 253–271.

BEDARD, J.H. 1991. Cumulate recycling and crustal evolution in the Bay of Islands ophiolite. *Journal of Geology* **99**, 225–249.

BLOOMER, S.H. & HAWKINS, J.W. 1987. Petrology and geochemistry of boninite series volcanic rocks from the Mariana trench. *Contributions to Mineralogy and Petrology* **97**, 361–377.

BURNS, L.E. 1985. The Border Ranges ultramafic and mafic complex, south central Alaska: cumulate fractionates of island arc volcancs. *Canadian Journal of Earth Sciences* **22**, 1020–1038.

CAMERON, W.E. 1985. Petrology and origin of primitive lavas from the Troodos ophiolite, Cyprus. *Contributions to Mineralogy and Petrology* **89**, 239–255.

ÇELİK, Ö.F., DELALOYE, M. & FERAUD, G. 2006. Precise ^{40}Ar-^{39}Ar ages from the metamorphic sole rocks of the Tauride Belt Ophiolites, southern Turkey: implications for the rapid cooling history. *Geological Magazine* (doi:10.1017/S0016756805001524).

CRAWFORD, A.J., BECCALUVA, L. & SERRI, G. 1981. Tectono-magmatic evolution of the west Philippine-Mariana region and the origin of boninites. *Earth and Planetary Scientific Letters* **54**, 346–356.

DICK, H.J.B. 1977. Partial melting in the Josephine peridotite. The effect on mineral composition and its consequence for geobarometry and geothermometry. *American Journal of Science* **277**, 801–832.

DICK, H.J.B. & BULLEN, T. 1984. Chromian spinel as a petrogenetic indicator in abyssal and alpine-type peridotites and spatially associated lavas. *Contributions to Mineralogy and Petrology* **86**, 54–76.

DİLEK, Y. & FLOWER, M.F.J. 2003. Arc-trench rollback and forearc accretion: 2. A model template for ophiolites in Albania, Cyprus, and Oman. *In:* DİLEK, Y. & ROBINSON, P.T. (eds), *Ophiolites in Earth History*. The Geological Society, London, Special Publications **218**, 43–69.

ELİTOK, Ö. 2001. Geochemistry and tectonic significance of the Şarkikaraağaç ophiolite in the Beyşehir-Hoyran nappes, SW Turkey. *In:* AKINCI, Ö., GÖRMÜŞ, M., KUŞÇU, M., KARAGÜZEL, R. & BOZCU, M. (eds), *Proceedings of 4th International Symposium on Eastern Mediterranean Geology (Süleyman Demirel University, Isparta), Turkey*. 181–196.

EMRE, H. 1986. *Orhaneli Ofiyolitinin Jeolojisi ve Petrolojisi [Geology and Petrology of Orhaneli Ophiolite]*. PhD Thesis, İstanbul University [in Turkish with English abstract, unpublished].

FLOWER, M.F.J., RUSSO, R.M., TAMAKI, K. & HOANG, N. 2001. Mantle contamination and the Izu-Bonin-Mariana (IBM), high-tide mark': evidence for mantle extrusion caused by Tethyan closure. *Tectonophysics* **333**, 9–34.

FLOYD, P.A. & WINCHESTER, J.A. 1978. Identification and discrimination of altered and metamorphosed volcanic rocks using immobile elements. *Chemical Geology* **21**, 291–306.

FLOYD, P.A. & CASTILLO, P.R. 1992. Geochemistry and petrogenesis of Jurassic ocean crust basalts, ODP Leg 129, Site 801. *In:* LARSON, R., LAUNCELAT, Y. *et al.* (eds), *Proceedings of ODP, Scientific Results* **129**, 361–388.

ŞENEL, M. 2001. *1/500.000 Scale Geological Map of Turkey*. General Directorate of Mineral Research and Exploration (MTA) Publications.

GÖNCÜOĞLU, M.C., TURHAN, N., ŞENTÜRK, K., ÖZCAN, A., UYSAL, Ş. & YALINIZ, M.K. 2000. A geotraverse across Northwestern Turkey: tectonic units of the Central Sakarya region and their tectonic evolution. *In:* BOZKURT, E., WINCHESTER, J.A. & PIPER, J.D.A (eds), *Tectonics and Magmatism in Turkey and the Surrounding Area*. Geological Society, London, Special Publications **173**, 139–163.

GREENBAUM, D. 1972. Magmatic processes at ocean ridges: Evidence from the Troodos massif, Cyprus. *Nature* **238**, 18–21.

GÜLTAŞLI, Ö.F. 1996. *Mineralogy, Petrography and Origin of Ultramafics in Orhaneli (Bursa) Ophiolite Complex*. MSc Thesis, Dokuz Eylül University [unpublished].

HARRIS, N.B.W., KELLER, S.P. & OKAY, A.İ. 1994. Post-collision magmatism and tectonics in northwest Turkey. *Contribution to Mineralogy and Petrology* **17**, 241–252.

HART, S.R., ERLANK, A.J. & KABLE, E.J.D. 1974. Sea floor basalt alteration: some chemical and Sr isotopic effects. *Contribution of Mineralogy and Petrography* **44**, 219–230.

HAWKINS, J.W., BLOOMER, S.H., EVANS, C.A. & MELCHIOR, J.T. 1984. Evolution of intraoceanic arc-trench systems. *Tectonophysics* **102**, 175–205.

HODGES, F.N. & PAPIKE, J.J. 1976. DSDP site 334: Magmatic cumulates from oceanic layer 3. *Journal of Geophysial Research* **81**, 4135–4151.

HUMPHRIS, S.E. & THOMPSON, G. 1978. Trace element mobility during hydrothermal alteration of oceanic basalts. *Geochimica et Cosmochimica Acta* **42**, 127–136.

IRVINE, T.N. 1967. Chromian spinel as a petrogenetic indicator. Part 2. Petrologic applications. *Canadian Journal of Earth Sciences* **4**, 71–103.

ISHIWATARI, A. 1994. Circum-Pacific Phanerozoic multiple ophiolite belts. *In:* ISHIWATARI, A., MALPAS, J. & ISHIZUKA, H. (eds), *Circum-Pacific Ophiolites (Proceedings of the 29th IGC, Kyoto, Part D).* VSP, Utrecht, 7–28.

ISHIWATARI, A., SOKOLOV, S.D. & VYSOTSKIY, S.V. 2003. Petrological diversity and origin of ophiolites in Japan and Far East Russia with emphasis on depleted harzburgite. *In:* DİLEK, Y. & ROBINSON, P.T. (eds), *Ophiolites in Earth History*. The Geological Society, London, Special Publications **218**, 597–619.

JACKSON, E.D., GREEN, H.W. & MOORES, E.M. 1975. The Vourinos ophiolite, Greece: Cyclic units of lineated cumulates overlying harzburgite tectonite. *Geological Society of America Bulletin* **86**, 390–398.

JENNER, G.A., DUNNING, G.R., MALPAS, J., BROWN, M. & BRACE, T. 1991. Bay of Islands and Little Port complexes, revisited: age, geochemical and isotopic evidence confirm suprasubduction zone origin. *Canadian Journal of Earth Sciences* **28**, 1635–1652.

JOHNSON, L.E. & FRAYER, P. 1990. The first evidence for MORB-like lavas from the outer Mariana forearc: geochemistry, petrography and tectonic implications. *Earth and Planetary Scientific Letters* **100**, 304–316.

JUTEAU, T., ERNEWEIN, M., REUBER, I., WHITECHURCH, H. & DAHL, R. 1988. Duality of magmatism in the plutonic sequence of the Sumail Nappe, Oman. *Tectonophysics* **51**, 107–135.

KAMENETSKY, V.S., CRAWFORD, A.J. & MEFFRE, S. 2001. Factors controlling chemistry of magmatic spinel: an empirical study of associated olivine, Cr-spinel and melt inclusions from primitive rocks. *Journal of Petrology* **42**, 655–671.

LISENBEE, A.L. 1972. *Structural Setting of the Orhaneli Ultramafic Massif near Bursa, Northwestern Turkey.* PhD Thesis, Pensylvania State University [unpublished].

MANAV, H., GÜLTEKİN, A.H. & UZ, B. 2004. Geochemical evidence for the tectonic setting of the Harmancık ophiolites, NW Turkey. *Journal of Asian Earth Sciences* **24**, 1–9.

NICOLAS, A. & JACKSON, M. 1972. Repartition en deux provinces des peridotites des chaines alpines longeant la mediteranée: implications géotectoniques. *Schweizische Mineralogische Petrographische Mitteilungen* **52**, 479–495.

OKAY, A.İ., TANSEL, İ. & TÜYSÜZ, O. 2001. Obduction, subduction and collision as reflected in the Upper Cretaceous–Lower Eocene sedimentary record of western Turkey. *Geological Magazine* **138**, 117–142.

OSMAN, A.F. 2004. *Tectonic Evolution of the Northern Oman Mountains: Outline and Discussion.* Field Trip Series **1**, United of Arabian Emirates.

ÖNEN, A.P. & HALL, R. 2000. Sub-ophiolite metamorphic rocks from NW Anatolia, Turkey. *Journal of Metamorphic Geology* **18**, 483–495.

ÖRGÜN, Y., GÜLTEKİN, A.H., ÇEVİK, E. & ÇOPUROĞLU, M. 2004. Mineralogic and geochemical characteristics of the Orhaneli dunite and its importance in point of olivine, Orhaneli-Bursa, Western Anatolia, Turkey. *5th International Symposium on Eastern Mediterranean Geology, Thessaloniki (Greece), Abstracts*, 1193–1196.

ÖZEN, H., ÇOLAKOĞLU, A., SAYAK, H., DÖNMEZ, C., TÜRKEL, A., ODABAŞI, İ., SARIFAKIOĞLU, E. & WINCHESTER, J.A. 2006. Erzincan'ın kuzeyindeki ofiyolitlere ait tektonit-kümülat kayaçların petrojenezine bir yaklaşım [The petrogenesis of tectonites and cumulate rocks from the ophiolites, north of Erzincan]. *59th Geological Congress of Turkey. Abstracts,* 100–101.

ÖZEN, H., ÇOLAKOĞLU, A., SAYAK, H., GÜLTAŞLI, Ö.F., BAŞTA, Ö. & SARIFAKIOĞLU, E. 2004. *Ofiyolitlere Bağlı Cevherleşmelerin Araştırılması [The Investigation of Ophiolite-related Mineralization].* Mineral Research and Exploration Institute of Turkey (MTA) Project no. **16B15**.

ÖZEN, H., SARIFAKIOĞLU, E., GÜLTAŞLI, Ö.F., BAŞTA, Ö., ÇOLAKOĞLU, A. & SAYAK, H. 2005. Orhaneli (Bursa) ofiyolitinin jeolojisi ve petrografik özellikleri [The geology and petographical characteristics of the Orhaneli ophiolite]. *58th Turkish Geological Congress of Turkey. Abstract,* 47–50.

ÖZKOÇAK, O. 1969. *Etude Géologique du massif ultrabasique D'Orhaneli et de sa proche bordure (Bursa-Turquie) sujet proposé par la faculté.* Pour otenir le titre de Docteur de l'Universite.

PALLISTER, J.S. & HOPSON, C.A. 1981. Samail ophiolite plutonic suite, field relations, phase variation, cryptic variation and layering, and a model of a spreading ridge magma chamber. *Journal of Geophysical Research* **86**, 2593–2644.

PANJASAWATWONG, Y., DANYUSHEVSKY, L.V., CRAWFORD, A.J. & HARRIS, K.L. 1997. An experimental study of the effects of melt composition on plagoclase-melt equilibria at 5 and 10 kbars: implications for the origin of magmatic high-An plagioclase. *Contributions to Mineralogy and Petrology* **118**, 420–432.

PARLAK, O., DELALOYE, M. & BİNGÖL, E. 1996. Mineral chemistry of ultramafic and mafic cumulates as an indicator of the arc-related origin of the Mersin ophiolite (southern Turkey). *Geologische Rundschau* **85**, 647–661.

PARLAK, O., HÖCK, V. & DELALOYE, M. 2002. The suprasubduction zone Pozantı-Karsantı ophiolite, southern Turkey: evidence for high-pressure crystal fractionation of ultramafic cumulates. *Lithos* **65**, 205–224.

PARLAK, O., YILMAZ, H. & BOZTUĞ, D. 2006. Origin and tectonic significance of the metamorphic sole and isolated dykes of the Divriği Ophiolite (Sivas, Turkey): Evidence for slab break-off prior to ophiolite emplacement. *Turkish Journal of Earth Sciences* **15**, 25–45.

PEARCE, J.A. 1982. Trace element characteristics of lavas from destructive plate boundaries. *In:* THORPE, R.S. (ed), *Andesites: Orogenic Andesites and Related Rocks*. John Wiley & Sons, Chichester, 525–548.

PEARCE, J.A. 1983. Role of the subcontinental lithosphere in magma genesis at active continental margins. *In:* HAWKESWORTH, C.J. & NORRY, M.J. (eds), *Continental Basalts and Xenoliths*. Shiva Publishing, Cheshire, 230–49.

PEARCE, J.A. 2003. Supra-subduction zone ophiolites: the search for modern analogues. *In:* DİLEK, Y. & NEWCOMB, S. (eds), *Ophiolite Concept and the Evolution of Geological Thought*. The Geological Society of America, Special Paper **373**, 269–295.

PEARCE, J.A. & CANN, J.R. 1973. Tectonic setting of basaltic volcanic rocks determined using trace element analyses. *Earth and Planetary Scientific Letters* **19**, 290–300.

PORTNYAGIN, M.V., MAGAKYAN, R. & SCHMINKE, H.U. 1996. Geochemistry variability of boninite magmas: avidence from magmatic inclusions in highly magnesian olivine from lavas of southwestern Cyprus. *Petrology* **4**, 231–246.

SARIFAKIOĞLU, E. & GÜLTAŞLI, Ö.F. 2003. Türkiye'deki Güney, Kuzey ve Toros ofiyolit kuşaklarına ait ultramafik-mafik kayaçların petrografik-jeokimyasal benzerlikleri [The petrographical and geochemistrical similarities of the ultramafic-mafic rocks from the southern, the northern and Taurus ophiolite belts in Turkey]. *20th Anniversary Geology Symposium (Süleyman Demirel University, Isparta), Abstracts* 158–159 [in Turkish with English abstract].

SARIFAKIOĞLU, E., ÖZEN, H., ÇOLAKOĞLU, A.O. & SAYAK, H. 2006. Sivrihisar (Eskişehir) kuzeybatısındaki Dağküplü ofiyolitini kesen alkalen volkanitlerin petrojenezine ve yaşına yeni bir yaklaşım [A new approach to the petrogenesis and age of the alkaline volcanics cutting through the Dağküplü ophiolite, Northwestern Sivrihisar (Eskişehir)]. *Mineral Research and Exploration Institute of Turkey (MTA) Bulletin* **132**, 75–90.

SAUNDERS, A.D. & TARNEY, 1984. Geochemical characteristics of basaltic volcanism within backarc basin. *In:* KOKELAAR, B.P. & HOWELLS, M.F. (eds), *Marginal Basin Geology*. Geological Society, London, Special Publications **16**, 59–76.

SHERVAIS, J.W. 1982. Ti-V plots and the petrogenesis of modern and ophiolitic lavas. *Earth and Planetary Scientific Letters* **59**, 101–118.

SMITH, R.E. & SMITH, S.E. 1976. Comments on the use of Ti, Zr, Y, Sr, K, P and Nb in classification of basaltic magmas. *Earth and Planetary Scientific Letters* **32**, 114–120.

STERN, R.J. & BLOOMER, S.H. 1992. Subduction zone infancy: Examples from the Eocene Izu-Bonin-Mariana and Jurassic California arcs. *Geological Society of America Bulletin* **104**, 1621–1636.

TANKUT, A. 1991. The Orhaneli massif, Turkey. *Ofioliti* **16**, 702–713.

THAYER, T.P. 1960. Some critical differences between alpine-type and stratiform peridotite-gabbro complexes. *21st International Geology Congress, Copenhagen* **13**, 247–259.

UMINO, S., YANAL, S., JAMAN, A.R., NAKAMURA, Y. & LIYAMA, J.T. 1990. The transition from spreading to subduction: Evidence from the Semail Ophiolite, northern Oman Mountains. *In:* MALPAS, J., MOORES, E.M., PANAYIOTOU, A. & XENOPHONTOS, C. (eds), *Ophiolites: Oceanic Crustal Analogues: Proceedings of the Symposium 'Troodos 1987'.* Geological Survey Department, Nicosia, Cyprus, 375–384.

UYSAL, İ., SADIKLAR, M.B., TARKIAN, M., KARSLI, O. & AYDIN, F. 2005. Mineralogy and composition of the chromitites and their platinum-group minerals from Ortaca (Muğla-SW Turkey): evidence for ophiolitic chromitite genesis. *Mineralogy and Petrology* **83**, 219–242.

WALKER, K.R., WARE, N.G. & LOVERING, J.F. 1973. Compositional variations in the Pyroxenes of the differentiated Palisades Sill, New Jersey. *Geological Society of American Bulletin* **84**, 89–110.

WILSON, M. 1989. *Igneous Petrogenesis: A Global Tectonic Approach.* Unwin Hyman Ltd., London.

WINCHESTER, J.A. & FLOYD, P.A. 1977. Geochemical discrimination of different magma series and their differentiation products using immobile elements. *Chemical Geology* **20**, 325–343.

WINCHESTER, J.A., VAN STAAL, C.R. & LANGTON, J.P. 1992. The Ordovician volcanics of the Elmtree-Belledune inlier and their relationships to volcanics of the northern Miramichi Highlands, New Brunswick. *Canadian Journal of Earth Sciences* **29**, 1430–1447.

WOOD, D.A., JORON, J.L. & TREUIL, M. 1979. A reappraisal of the use of the trace elements to classify and discriminate between magma series erupted in different tectonic settings. *Earth and Planetary Scientific Letters* **45**, 101–118.

YALINIZ, K.M., FLOYD, P.A. & GÖNCÜOĞLU, M.C. 1996. Suprasubduction zone ophiolites of Central Anatolia: geochemical evidence from the Sarıkaraman Ophiolite, Aksaray, Turkey. *Mineralogical Magazine* **60**, 697–710.

ZHOU, M.F. & ROBINSON, P.T. 1994. High-chromium and high-aluminum podiform chromitites, western China: relationship to partial melting and melt/rock interaction in the upper mantle. *International Geological Review* **36**, 678–686.